

ผลของความบกพร่องบนพื้นผิวของไทเทเนียมต่อความว่องไวในการเร่งปฏิกิริยาโดยใช้แสง

สำหรับแยกสลายน้ำเป็นไฮโดรเจน



นางสาววราพร นัครไพศาลสกุล

สถาบันวิทยบริการ
จุฬาลงกรณ์มหาวิทยาลัย
วิทยานิพนธ์นี้เป็นส่วนหนึ่งของการศึกษาตามหลักสูตรปริญญาวิศวกรรมศาสตรมหาบัณฑิต

สาขาวิชาวิศวกรรมเคมี ภาควิชาวิศวกรรมเคมี

คณะวิศวกรรมศาสตร์ จุฬาลงกรณ์มหาวิทยาลัย

ปีการศึกษา 2549

ลิขสิทธิ์ของจุฬาลงกรณ์มหาวิทยาลัย

EFFECT OF SURFACE DEFECT OF TITANIUM DIOXIDE ON
PHOTOCATALYTIC ACTIVITY FOR WATER DECOMPOSITION
TO HYDROGEN



Miss Waraporn Chatpaisalsakul

สถาบันวิทยบริการ

จุฬาลงกรณ์มหาวิทยาลัย

A Thesis Submitted in Partial Fulfillment of the Requirements
for the Degree of Master of Engineering Program in Chemical Engineering

Department of Chemical Engineering

Faculty of Engineering

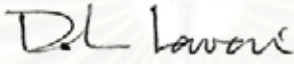
Chulalongkorn University

Academic Year 2006

Copyright of Chulalongkorn University

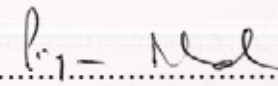
Thesis Title EFFECT OF SURFACE DEFECT OF TITANIUM
DIOXIDE ON PHOTOCATALYTIC ACTIVITY FOR
WATER DECOMPOSITION TO HYDROGEN
By Miss Waraporn Chatpaisalsakul
Field of Study Chemical Engineering
Thesis Advisor Professor Piyasan Prasertthdam, Dr.Ing.

Accepted by the Faculty of Engineering, Chulalongkorn University in Partial
Fulfillment of the Requirements for the Master's Degree



..... Dean of the Faculty of Engineering
(Professor Direk Lavansiri, Ph.D.)

THESIS COMMITTEE


..... Chairman
(Assistant Professor Bunjerd Jongsomjit, Ph.D.)


..... Thesis Advisor
(Professor Piyasan Prasertthdam, Dr.Ing.)


..... Member
(Assistant Professor Okorn Mekasuwandumrong, D.Eng.)


..... Member
(Akawat Sirisuk, Ph.D.)

วราพร ฉัตรไพศาลสกุล : ผลของความบกพร่องบนพื้นผิวของไทเทเนียมต่อความว่องไวในการเร่งปฏิกิริยาโดยใช้แสงสำหรับแยกสลายน้ำเป็นไฮโดรเจน (EFFECT OF SURFACE DEFECT OF TITANIUM DIOXIDE ON PHOTOCATALYTIC ACTIVITY FOR WATER DECOMPOSITION TO HYDROGEN) อ.ที่ปรึกษา: ศ.ดร. ปิยะสาร ประเสริฐธรรม, 92 หน้า.

การศึกษาผลของการใช้งานความบกพร่องบนพื้นผิวของตัวเร่งปฏิกิริยาไทเทเนียมต่อความว่องไวในการเร่งปฏิกิริยาโดยใช้แสงสำหรับแยกสลายน้ำเป็นไฮโดรเจน โดยผลึกขนาดนาโนเมตรของตัวเร่งปฏิกิริยาไทเทเนียมได้จากการเตรียมด้วยวิธีโซโวเทอร์มอล จากนั้นทำการปรับปรุงพื้นผิวของตัวเร่งปฏิกิริยาไทเทเนียมที่ได้ โดยการนำไปเผาแล้วทำให้เย็นตัวอย่างรวดเร็วในตัวกลางที่เป็นสถานะของเหลวและสถานะก๊าซ โดยตัวกลางสถานะของเหลว คือ น้ำที่อุณหภูมิห้อง น้ำที่อุณหภูมิ 373 เคลวิน ไฮโดรเจนเปอร์ออกไซด์ที่อุณหภูมิห้อง และ ไฮโดรเจนเปอร์ออกไซด์ที่อุณหภูมิ 373 เคลวิน และสถานะก๊าซ คือ อากาศที่อุณหภูมิ 77 เคลวิน อากาศที่อุณหภูมิห้อง และอากาศที่อุณหภูมิ 373 เคลวิน โดยพบว่าทำให้ตัวเร่งปฏิกิริยาไทเทเนียมเย็นตัวอย่างรวดเร็วในทุกๆ ตัวกลางที่ศึกษานั้น ไม่มีผลต่อการเปลี่ยนแปลงของขนาดผลึกและพื้นที่ผิวของตัวเร่งปฏิกิริยาไทเทเนียม แต่พบว่าทำให้เกิดความบกพร่องบนพื้นผิวของตัวเร่งปฏิกิริยาไทเทเนียม โดยในทุกตัวกลางพบว่าที่อุณหภูมิต่ำกว่าจะทำให้เกิดความบกพร่องบนพื้นผิวของตัวเร่งปฏิกิริยาไทเทเนียมได้มากกว่าที่อุณหภูมิสูง นอกจากนั้นจากการใช้งานความบกพร่องบนพื้นผิวของตัวเร่งปฏิกิริยาไทเทเนียมในการเร่งปฏิกิริยาโดยใช้แสงสำหรับแยกสลายน้ำเป็นไฮโดรเจนยังพบว่า ตัวเร่งปฏิกิริยาที่มีปริมาณความบกพร่องบนพื้นผิวมาก จะมีประสิทธิภาพในการเร่งปฏิกิริยาได้ดีกว่าตัวเร่งปฏิกิริยาที่มีปริมาณความบกพร่องบนพื้นผิวน้อย นอกจากนี้พบว่าไฮดรอกซิลกรุปบนพื้นผิวของตัวเร่งปฏิกิริยามีผลต่อเวลาเริ่มต้นในการเกิดปฏิกิริยา

ภาควิชา.....วิศวกรรมเคมี.....

สาขาวิชา.....วิศวกรรมเคมี.....

ปีการศึกษา.....2549.....

ลายมือชื่อนิสิต.....ศ.ดร. ฉัตรไพศาลสกุล.....

ลายมือชื่ออาจารย์ที่ปรึกษา..........

4870456921 : MAJOR CHEMICAL ENGINEERING
 KEY WORD: TITANIUM DIOXIDE / SURFACE DEFECT / PHOTOCATALYTIC
 / WATER DECOMPOSITION

WARAPORN CHATPAISALSAKUL: EFFECT OF SURFACE DEFECT
 OF TITANIUM DIOXIDE ON PHOTOCATALYTIC ACTIVITY FOR
 WATER DECOMPOSITION TO HYDROGEN. THESIS ADVISOR: PROF.
 PIYASAN PRASERTHDAM, Dr.Ing., 92 pp.

Effects of TiO_2 surface defects on photocatalytic activity for water decomposition to hydrogen are also investigated. Nanocrystalline titanium dioxide was prepared using the solvothermal method. Obtained titanium dioxide powder was treated to modify the surface properties by quenching in various media. For quenching in liquid phase medias, water at room temperature and 373 K, hydrogen peroxide at room temperature and 373 K were selected. For quenching in gas phase media, air at room temperature, 373 K and 77 K were selected. It is also found that quenching titanium dioxide catalysts in various media is not significantly differences in the crystallites size and BET surface area, but it is also found that quenching immediately after calcined was increasing amount of Ti^{3+} on surface of catalyst and exhibited increasing photocatalytic activity. Quenching in a similar medium, TiO_2 quenched in cooler media exhibited higher photocatalytic activity than those quenched in hotter ones. For room temperature quenching, the photocatalytic activities of TiO_2 quenched in air exhibited higher activity than those quenched in 30 %wt H_2O_2 and H_2O , respectively. There were observed that start of the reaction because of bridging hydroxyl group and water on the TiO_2 surface.

Department.....Chemical Engineering..... Student's signature.....Waraporn Chatpaisalsakul.

Field of study...Chemical Engineering.....Advisor's signature.....

Academic year2006.....

ACKNOWLEDGEMENTS

The author would like to express her sincere gratitude and appreciation to her advisor, Professor Piyasan Prasertdam , for her invaluable suggestions, encouragement during her study, useful discussions throughout this research and especially, giving her the opportunity to present her research at RSCE conference in Singapore. In addition, the author would also be grateful to Assistant Professor Bunjerd Jongsomjit, as the chairman, Assistant Professor Okorn Mekasuwandumrong and Dr. Akawat Sirisuk as the members of the thesis committee. The financial supports of the Thailand Research Fund (TRF), TJTTP-JBIC, and the Graduate School of Chulalongkorn University are gratefully acknowledged.

Most of all, the author would like to express her highest gratitude to her parents who always pay attention to her all the times for suggestions and listen her complain. The most success of graduation is devoted to my parents.

The author would like to acknowledge with appreciation to Assistant Professor Okorn Mekasuwandumrong, Mr. Kongkiat Suriye, Miss Wilasinee Kongsuebchart and Mr. Piyawat Supphasrironrojaroen for their kind suggestions on her research without hesitation.

Finally, the author wishes to thank the members of the Center of Excellence on Catalysis and Catalytic Reaction Engineering, Department of Chemical Engineering, Faculty of Engineering, Chulalongkorn University for friendship. To the many others, not specifically named, who have provided her with support and encouragement, please be assured that she thinks of you.

CONTENTS

	Page
ABSTRACT (IN THAI)	iv
ABSTRACT (IN ENGLISH)	v
ACKNOWLEDGMENTS	vi
CONTENTS	vii
LIST OF TABLES	x
LIST OF FIGURES	xi
CHAPTER	
I INTRODUCTION	1
II LITERATURE REVIEWS	5
2.1 Photocatalysis on titanium dioxide.....	5
2.2 Surface defect.....	7
2.3 Effect of surface defect on photocatalytic reaction.....	8
III THEORY	10
3.1 Titanium (IV) oxide.....	10
3.2 Solvothermal method.....	12
3.3 Quenching process.....	13
3.4 Defect structure of crystal material.....	16
3.5 Photocatalytic reaction.....	18
3.6 Mechanisms of semiconductor photocatalytic water-splitting or hydrogen production.....	22
IV EXPERIMENTS	25
4.1 Chemicals.....	25
4.2 Equipment.....	26
4.2.1 Autoclave reactor.....	26
4.2.2 Temperature program controller.....	27
4.2.3 Electrical furnace (Heater).....	27
4.2.4 Gas controlling system.....	27
4.3 Catalyst Preparation.....	28
4.3.1 Preparation of Titanium dioxide nanoparticles.....	28

	Page
4.3.2 Modified Titanium dioxide nanoparticles.....	28
4.4 Photocatalytic Activity Evaluations.....	29
4.5 Catalyst Characterization.....	31
4.5.1 X-ray diffraction analysis (XRD).....	31
4.5.2 Surface area measurement.....	31
4.5.3 Temperature programmed desorption (TPD).....	31
4.5.4 Electron spin resonance spectroscopy (ESR).....	32
4.5.5 UV-visible absorption spectroscopy (UV-Vis).....	32
4.5.6 Thermal gravimetric Analysis (TGA).....	32
4.5.7 Fourier-Transform Infrared Spectroscopy (FT-IR)	32
V RESULTS AND DISCUSSION.....	33
5.1 Formation of Titanium Dioxide.....	33
5.2. Structure and surface properties of TiO ₂ quenched in different media.....	34
5.2.1 X-ray diffraction analysis (XRD).....	34
5.2.2 Surface area measurement.....	36
5.2.3 The characteristics of surface adsorption site of TiO ₂ samples.....	37
5.2.4 Electron spin resonance spectroscopy (ESR).....	40
5.3 Effect of quenching process on surface defect of TiO ₂	42
5.3.1 Effect of temperature for the quenching media on surface defect.....	42
5.3.2 Effect of different the quenching media on surface Defect.....	47
5.4 Photocatalytic activity of the TiO ₂ quenched in various media.	51
5.4.1 Effect of temperature for the quenching media on photocatalytic activity.....	55
5.4.2 Effect of different the quenching media on photocatalytic activity.....	58
5.5 Photocatalytic Reaction.....	61
5.5.1 UV-visible absorption measurement.....	62

	Page
5.5.2 Thermal gravimetric Analysis (TGA).....	64
5.5.3 Fourier-Transform Infrared Spectroscopy (FT-IR)	65
VI CONCLUSIONS AND RECOMMENDATION.....	67
6.1 Conclusions.....	67
6.2 Recommendation.....	68
REFERENCES.....	69
APPENDICES.....	73
APPENDIX A: CALCULATION OF THE CRYSTALLITE SIZE.	74
APPENDIX B: CALIBRATION CURVES.....	77
APPENDIX C: DETERMINATION OF Ti³⁺ SURFACE DEFECT FROM ESR MEASUREMENT.....	79
APPENDIX D: DATA OF CHARACTERIZATION OF Ti³⁺ SURFACE DEFECT FROM TEMPERATURE PROGRA DESORPTION...	80
APPENDIX E: DATA OF PHOTOCATALYTIC REACTION FOR WATER DECOMPOSITION TO HYDROGEN.....	86
APPENDIX F: LIST OF PUBLICATIONS.....	89
VITA.....	92

LIST OF TABLES

TABLE		Page
3.1	Comparison of properties of anatase, brookite, and rutile.....	11
4.1	Chemical used in the experiment.....	25
4.2	Operating condition for gas chromatograph.....	30
5.1	The crystallite size and BET surface area of titanium dioxide...	36
5.2	Ratios of peak areas of Ti^{3+}/Ti^{4+} were also determined from the CO_2 -TPD measurements.....	39
5.3	The amount of Ti^{3+} surface defect of TiO_2 were also determined from the ESR measurements.....	41
5.4	Comparing of the amount of Ti^{3+} surface defects of TiO_2 dependent in terms of the thermal shock effect were also determined from the CO_2 -TPD and the ESR measurements.....	45
5.5	Comparing of the amount of Ti^{3+} surface defects of TiO_2 dependent on the % water in quenching media were also determined from the CO_2 -TPD and the ESR measurements.....	49
5.6	The band gap energy of TiO_2 quenched in various media.....	51
5.7	The band gap energy of TiO_2 quenched in various media.....	63
B.1	The operating conditions for gas chromatograph.....	77
C.1	The relative amount of Ti^{3+} surface defects of titanium dioxide quenched in various quenching media.....	79
D.1	The intensity peak of titanium dioxide quenched in various quenching media.....	80
E.1	The data and results of photocatalytic reaction for water decomposition to hydrogen of titanium dioxide quenched in various media.....	86

LIST OF FIGURES

FIGURE		Page
3.1	Crystal structures of Titanium dioxide in rutile, anatase and brookite.....	10
3.2	Cation and anion charge-balanced Shottky defects in NaCl. The metal atoms are smaller than the non-metal atoms. The defect consists of vacancies on both metal and non-metal sites.	17
3.3	Pair of charge-balanced Frenkel defects in AgI. The metal atoms are smaller than the non-metal atoms. The defects consist of equal numbers of vacancies on either the metal or non-metal or non-metal sub-lattice and interstitial ions of the same type.....	18
3.4	Band-gap diagram (formation of holes (h+) and electrons (e-) upon UV irradiation of semiconductor surface).....	19
3.5	Main processes occurring on a semiconductor particle.....	20
3.6	Energy diagram for typical semiconductors.....	21
3.7	Mechanism of TiO ₂ photocatalytic water splitting for hydrogen production.....	23
4.1	Autoclave reactor.....	26
4.2	Diagram of the reaction equipment for the catalyst preparation.	27
4.3	Experiment set-up of photochemical reactor.....	30
5.1	Mechanism of reaction in toluene for the titanium dioxide.....	33
5.2	The XRD patterns of the TiO ₂ obtained from quenching in various media.....	35
5.3	Thermal desorption spectra for CO ₂ adsorbed on TiO ₂ quenched in different media.....	38
5.4	Ratios of peak areas of Ti ³⁺ /Ti ⁴⁺ and various quenching media.	39

FIGURE	Page
5.5 ESR spectra of TiO ₂ quenched in different media.....	40
5.6 Intensity of Ti ³⁺ surface defects per surface area and various quenching media.....	41
5.7 Thermal desorption spectra for CO ₂ adsorbed on TiO ₂ quenched in air at different temperature.....	43
5.8 Thermal desorption spectra for CO ₂ adsorbed on TiO ₂ quenched in 30% wt hydrogen peroxide at different temperature.....	43
5.9 Thermal desorption spectra for CO ₂ adsorbed on TiO ₂ quenched in water at different temperature.....	44
5.10 Ratios of peak areas of Ti ³⁺ /Ti ⁴⁺ and different temperature in various media.....	45
5.11 Intensity of Ti ³⁺ surface defects per surface area and different temperature in various media.....	46
5.12 Thermal desorption spectra for CO ₂ adsorbed on TiO ₂ quenched in different the quenching media at room temperature.....	48
5.13 Thermal desorption spectra for CO ₂ adsorbed on TiO ₂ quenched in different the quenching media at 373 K.....	48
5.14 Ratios of peak areas of Ti ³⁺ /Ti ⁴⁺ and % water in air, 30% wt H ₂ O ₂ and H ₂ O.....	50
5.15 Intensity of Ti ³⁺ surface defects per surface area and % water in air, 30% wt H ₂ O ₂ and H ₂ O.....	50
5.16 Results of photocatalytic testing comparing the activities of TiO ₂ quenched in different media.....	53
5.17 Results of photocatalytic testing comparing the activities of TiO ₂ quenched in different media.....	54
5.18 Results of photocatalytic testing comparing the activities of TiO ₂ quenched in different temperature of the quenching media in air.....	56

FIGURE	Page
5.19 Results of photocatalytic testing comparing the activities of TiO ₂ quenched in different temperature of the quenching media in hydrogen peroxide.....	56
5.20 Results of photocatalytic testing comparing the activities of TiO ₂ quenched in different temperature of the quenching media in water.....	57
5.21 Results of photocatalytic testing comparing the activities of TiO ₂ quenched in different the quenching media at room temperature.....	59
5.22 Results of photocatalytic testing comparing the activities of TiO ₂ quenched in different the quenching media at 373 K.....	59
5.23 Results of photocatalytic testing comparing the activities of TiO ₂ quenched in various media and % water of air, 30% wt H ₂ O ₂ and H ₂ O.....	60
5.24 Results of photocatalytic testing comparing the activities of TiO ₂ quenched in different media.....	61
5.25 The UV- vis spectra of TiO ₂ quenched in different media.....	62
5.26 The TGA profiles of TiO ₂ quenched in different media.....	64
5.27 The IR spectra of TiO ₂ quenched in different media.....	65
A.1 The 101 diffraction peak of titanium dioxide for calculation of the crystallite size.....	75
A.2 The plot indicating the value of line broadening due to the equipment. The data were obtained by using α -alumina as standard.....	76
B.1 The calibration curve of hydrogen.....	78
D.1 Thermal desorption spectra for CO ₂ adsorbed on TiO ₂ quenched in air at 77 K from integrator.....	82

FIGURE	Page
D.2 Thermal desorption spectra for CO ₂ adsorbed on TiO ₂ quenched in air at RT from integrator.....	82
D.3 Thermal desorption spectra for CO ₂ adsorbed on TiO ₂ quenched in air at 373 K from integrator.....	83
D.4 Thermal desorption spectra for CO ₂ adsorbed on TiO ₂ quenched in 30% wt H ₂ O ₂ at RT from integrator.....	83
D.5 Thermal desorption spectra for CO ₂ adsorbed on TiO ₂ quenched in 30% wt H ₂ O ₂ at 373 K from integrator.....	84
D.6 Thermal desorption spectra for CO ₂ adsorbed on TiO ₂ quenched in H ₂ O at RT from integrator.....	84
D.7 Thermal desorption spectra for CO ₂ adsorbed on TiO ₂ quenched in H ₂ O at 373 K from integrator.....	85
D.8 Thermal desorption spectra for CO ₂ adsorbed on TiO ₂ from integrator.....	85

CHAPTER I

INTRODUCTION

It has been known that Titanium dioxide is a material of great interest. It is well-known for its applications in the field of photocatalytic reactions, catalyst support, and as sensors. Due to its strong oxidizing power of its holes, high photostability, and redox selectivity, titanium dioxide is one of the most popular and promising catalysts in photocatalytic applications for environmental remediation (Herrmann et al. 2002). In general, a photocatalytic reaction involves various processes on the titanium dioxide surface such as oxidation reaction by photo-generated holes, reduction reaction by photo-generated electrons, diffusion of electrons and holes, and electron-hole recombination. Due to its tremendous technological importance, surface properties of titanium dioxide have been extensively investigated in order to understand its photocatalytic properties. Some success in enhancing the photocatalytic activity has been achieved by several methods, such as using nano-sized semiconductor crystallites instead of bulk materials and modifying photocatalysts by sulfation (Deng et al. 2002), reduction with hydrogen (Liu et al. 2003), halogenation (Amama et al. 2002). These methods can greatly improve the separation rate of photo-induced charge carriers in semiconductor photocatalysts so that the photocatalytic activity increases.

Nanocrystalline titanium dioxide is usually prepared by sol-gel (Wang and Ying 1999), gas-synthesis, and solvothermal method. Although the sol-gel method is widely used to prepare nanometer titanium dioxide, calcination process will inevitably cause the grain growth and reduction in specific surface area of particles and even induce phase transformation. Solvothermal synthesis, in which chemical reactions can occur in aqueous or organic media under the self-produced pressure at low temperature, (usually lower than 250 °C) can solve those problems encountered during sol-gel process. Therefore, we would like to synthesis nano-sized titanium dioxide using solvothermal method.

Titanium dioxide always exists structural defects on the surface and inside the titanium dioxide particles (Torimoto et al. 1996). Although, the bulk defect is important factor to control level of perfect crystal, the surface defect is more important than bulk structure in field of surface science such catalyst and support. It has been known that surface defects play a fundamental role in the interaction of molecules with oxide surfaces, since defects act as active sites for the adsorption and dissociation of molecules on the surface (Diebold 2003). In titanium dioxide surfaces, these defects, mainly Ti^{3+} species (oxygen vacancies), play an important role in the photo-oxidation of organic species on the titanium dioxide photocatalyst (Shklover et al. 1997). The use of a variety of techniques including X-ray photoelectron spectroscopy (XPS) (Diebold 2003), O_2 photodesorption (Rusu and Yates 1997), electron spin resonance (ESR) (Nakaoka and Nosaka 1997) and CO_2 -temperature programmed reduction (TPD) (Thompson et al. 2003) can monitor the surface defect of titanium dioxide. Some of the common methods to create defect sites on the titanium dioxide surface are annealing at temperatures above 400 K, ion bombardment, electron beam or UV exposure (Shultz et al. 1995), and reducing with hydrogen. These methods are very complicated techniques because its use many equipment and high cost for setup to commercial scale. An alternative pre-treatment technique for create defect sites on titanium dioxide surface is quenching process. This possible an effective method for improve photocatalytic activity of the titanium dioxide because in the literature find the variety of the surface defects, strains and reconstructions caused by the process of annealing or quenching (Henderson 1996).

For application of surface defect on titanium dioxide, there are only few applications such as gas-adsorption (CO , CO_2 , H_2 , and H_2O) (Liu et al. 2002; Tilocca and Selloni 2004) and photocatalytic. In the latter, it have only a theory of trapping site of surface defect, but no experimental data have proved on effect of surface defect on the photocatalytic activity so far. It has been known that, the best applications of titania in field of catalyst are photocatalyst and support (strong-metal support). Therefore, in this work, we would like to study application of surface defect of titanium dioxide in field of photocatalyst.

Many studies have been reported on the relations between crystallographic structure and surface properties and the effect of these properties on the photocatalytic properties (Machado and Santana 2005). Thus, the objective of this work was to investigate the influence of quenching processes of titanium dioxide on photocatalytic activity for water decomposition to hydrogen.

From the beginning of the last century, the scientific community has recognized hydrogen as a potential source of fuel. Current uses of hydrogen are generally in industrial processes, as well as in rocket fuels and spacecraft propulsion. With further research and development, this hydrogen fuel is believed to be able to effectively serve as an alternative source of energy for generating electricity and fueling motor vehicles. Therefore, it is of significant interest in the development of fuel processing technologies and catalysts/photocatalysts to produce hydrogen from an abundantly available resource; water.

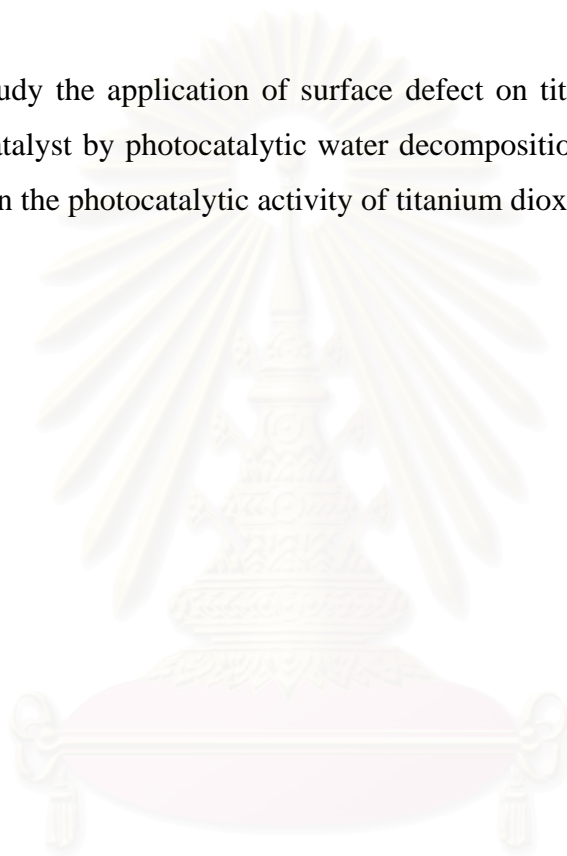
Efforts are currently underway to improve photochemical methods for hydrogen production. In this research, the main purpose is to photocatalytic performance of water decomposition to hydrogen have been studied by titanium dioxide powder photocatalyst, Effects of surface defect on the photocatalytic activity of titanium dioxide are also investigated. The scopes of this study are as following:

1. To study the effect of quenching processes on photocatalytic activity and surface defect of nanocrystalline titanium dioxide prepared by solvothermal method.

- Nanocrystalline titanium dioxide was prepared using the solvothermal method. Obtained titanium dioxide powder was treated to modify the surface properties by a rapid quenching in various media.

- For quenching in liquid phase media, water at room temperature and 373 K, hydrogen peroxide at room temperature and 373 K were selected. For quenching in gas phase media, air at room temperature, 373 K and 77 K were selected.

2. To study the application of surface defect on titanium dioxide catalyst in field of photocatalyst by photocatalytic water decomposition to hydrogen. Effects of surface defect on the photocatalytic activity of titanium dioxide are also investigated.



สถาบันวิทยบริการ
จุฬาลงกรณ์มหาวิทยาลัย

CHAPTER II

LITERATURE REVIEWS

Titanium dioxide is a useful material for many applications. Therefore, several studies have addressed the relationship between bulk/surface structures and its properties such as chemical adsorption, photocatalytic reaction, metal-support catalyst, and crystal growth. Moreover, the several researches about photocatalytic decomposition of water to hydrogen were discussed, too.

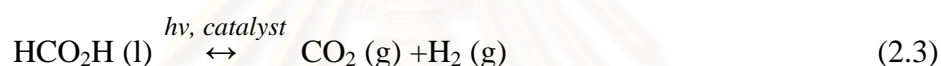
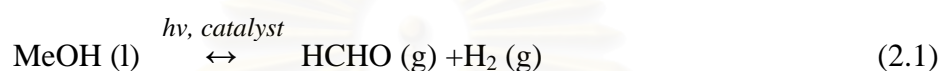
2.1 Photocatalytic decomposition of water to hydrogen on titanium dioxide

Titanium dioxide has drawn tremendous attention for its potential applications in photocatalysis in different fields, because of its high stability and favorable band-gap energy. For hydrogen production from water, many studies have concluded that direct photodecomposition of water into hydrogen and oxygen has a very low efficiency due to rapid reverse reaction. A much higher hydrogen production rate can be obtained by addition of a “sacrificial reagent,” such as alcohols, carbohydrates solid carbons, sulfide, etc (Wu et al. 2004). This suggests that photoexcited electrons and holes can be efficiently separated in a small semiconductor particle and that they are available for an irreversible chemical reaction, oxidization of sacrificial reagent. It is, therefore, inferred that a low efficiency of photodecomposition of water into hydrogen and oxygen is mainly due to a rapid reverse reaction between produced hydrogen and oxygen. Thus, a critical problem to be resolved for realizing the up-hill reaction efficiently is how to prevent such thermodynamically favored reverse reaction (Moon et al. 2000).

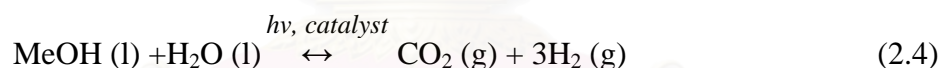
Of particular interest in these intercalated nanoparticles was the production of hydrogen from water containing a sacrificial agent under visible light irradiation with quantum yields as high as 10%. This might be attributable to the ease in donating lone-pair electrons to the valence band hole upon the photocatalyst excitation.

Compared to other types of sacrificial reagents among the alcohol series itself, methanol was found to be the most effective and strongest sacrificial reagent to yield the highest photocatalytic H₂ evolution activity.

For hydrogen production from a water/methanol solution, depending on reaction conditions and on whether metal catalyst used, the reaction could proceed either stepwise, involving stable intermediates, such as aldehydes and acids:



as suggested by Sakata et al. (Sakata et al. 1982), or in one-step on catalyst surface to give the overall reaction:



as suggested by Chen et al. (Chen et al. 1999). Hydrogen is produced in all of these steps (Wu, 2004).

The photocatalytic performance of titanium dioxide is well known to depend not only on its bulk energy band structure but, to a great extent, on the surface property. The type and density of surface state are affected by, among others, the synthesis process. Crystalline titanium dioxide has typically been calcined and/or crystallized in oxidizing atmospheres, such as air and oxygen. The effect of the so-called “inert” atmospheres, such as N₂, Ar, and vacuum, has mostly been overlooked. In the present work, we studied the effect of calcinations atmospheres, including Ar, air, N₂, H₂ and vacuum (5×10^{-3} Torr), on the photocatalytic properties of titanium dioxide, using photocatalytic H₂ production from methanol/water solution as the chemical probe. In summary, calcination atmosphere has been found to have

significant effects on the photocatalytic activity of titanium dioxide in hydrogen production from methanol/water solution. Calcination in either hydrogen or vacuum results in a high defect density and low surface hydroxyl coverage, giving low activity. Calcination in Ar, in contrast, enhances visible-light excitation and high hydroxyl coverage, leading to high activity (Wu et al. 2004).

2.2 Surface Defect

The structure of single-crystal titanium dioxide surfaces has been extensively. On the fully oxidized, defect-free titanium dioxide surface, all the surface Ti cations are in the 4+ oxidation state and are 5-fold coordinated to oxygen anions. Heating the surface to high temperatures induces desorption of surface oxygen, producing oxygen vacancies. One missing oxygen atom at the bridging-O site leaves two subsurface Ti^{3+} sites exposed. It is the relative ease in producing such defect sites that makes the titanium dioxide surface more reactive than other oxides, such as Al_2O_3 and SiO_2 , which are also commonly used as catalyst supports. The defective titanium dioxide means that the titanium dioxide is in chemical non-stoichiometry where the ratio of Ti to O within titanium dioxide is less than 2. Therefore, a measurement of degree of non-stoichiometry of titanium dioxide is considered to give more important information to help understand the intrinsic property of titanium dioxide (Kim et al. 2003b). Therefore, it has many studies in this topic because it easily detects using many techniques such as XPS, STM, Gas-adsorption, and ESR.

A new development to create the surface defect (Ti^{3+}) on TiO_2 was reported by Suriye et al. (Suriye et al. 2007) and compared to the common methods which must prepare the crystalline TiO_2 in the first step prior, and then create the surface defect in the second step. The surface defect creation was performed in the first step coinciding with the crystalline TiO_2 preparation using the sol-gel method. The creation was performed by varying the amounts of oxygen fed during calcination. Based on the CO_2 -temperature programmed desorption (CO_2 -TPD) and electron spin resonance (ESR) results, the surface defect (Ti^{3+}) substantially increased with the

amount of oxygen fed. Moreover, the samples resulting from calcination were used as photocatalysts for ethylene decomposition.

From using CO₂-TPD and ESR, it was found that the surface defect density (Ti³⁺) could be increased by increasing the amount of oxygen fed. Also, the increased Ti³⁺ amounts did not result from the reduction of Ti⁴⁺ to Ti³⁺ due to low calcination temperature used in the absence of hydrogen. They propose that the removal of the surface hydroxyl group when exposed to increased oxygen concentration accounts for the formation of the surface defect (Ti³⁺). Considering the photoactivities of TiO₂, it revealed that the conversion of ethylene increased with increasing surface defect because the Ti³⁺ play significant roles as the active sites for O₂ adsorption and also as sites for trapping photo-electrons to prevent the e⁻ h⁺ recombination process. It should be further noted that the surface area of TiO₂ did not control its photoactivity, but its surface defect did.

2.3 Effect of surface defect on photocatalytic reaction

The photocatalytic activity of titanium dioxide is greatly influenced by its crystal structure, particle size, surface properties, surface area and porosity. In case of surface defect (Park et al. 1999) reported that if the surface defects (Ti³⁺) are present to trap the electron, an e⁻-h⁺ recombination can be prevented, then the subsequent reactions caused by the electrons and holes may be dramatically enhanced. (Liu et al. 2003) proposed mechanism of surface defect on photocatalytic reactions. They concluded that both oxygen vacancies and Ti³⁺ species act as hole traps, and when they combine with photogenerated holes, they become charged species. At the same time, oxygen acts as an electron trap. The trapped holes transfer to the organic substrate leading to a degradation reaction and the charged defects recover to their original state of oxygen vacancies and Ti³⁺. However, no experimental data have proved on effect of Ti³⁺ on the photocatalytic activity so far.

Studied nano-TiO₂ powders with average crystallite sizes in the range of 9–15 nm were synthesized by the solvothermal method. The effect of crystallite size on the amount of surface defects on TiO₂ was investigated by means of X-ray diffraction (XRD), N₂ physisorption, temperature-programmed desorption of CO₂, and ESR spectroscopy. Photocatalytic activities of the TiO₂ powders were determined from a gas-phase decomposition of ethylene under UV irradiation. They found to the photocatalytic activities of the various TiO₂ crystallite sizes are evidently different; ethylene conversions increased with increasing TiO₂ crystallite sizes. It can be correlated to the different amounts of Ti³⁺ defects on TiO₂ samples, in which the higher the amount of Ti³⁺ present in TiO₂, the higher photocatalytic activity obtained (Kongsuebchart et al. 2006).



สถาบันวิทยบริการ
จุฬาลงกรณ์มหาวิทยาลัย

CHAPTER III

THEORY

3.1 Titanium (IV) oxide

Titanium (IV) oxide (Meng Ni 2005) belongs to the family of transition metal oxides. Titanium dioxide has received a great deal of attention due to its chemical stability, non-toxicity, low cost, and other advantageous properties. Titanium dioxide is also used in catalytic reactions acting as a promoter, a carrier for metals and metal oxides, an additive, or as a catalyst. The structures of rutile, anatase and brookite can be discussed in terms of $(\text{TiO}_2)^{6-}$ octahedrals. The three crystal structures differ by the distortion of each octahedral and by the assembly patterns of the octahedral chains (Figure 3.1). These crystals are substantially pure titanium (IV) oxide but usually amount of impurities, e.g., iron, chromium, or vanadium, which darken them. Comparison of typical physical properties of the three varieties is displayed in Table 3.1

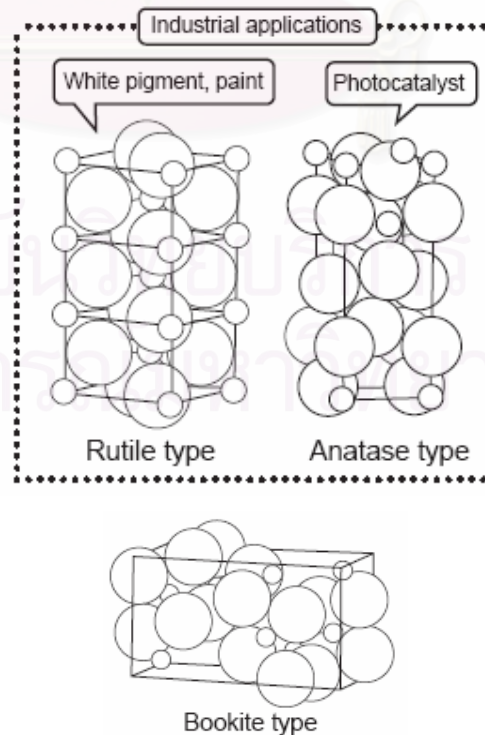


Figure 3.1 Crystal structures of Titanium dioxide in rutile, anatase and brookite.

Rutile is the most stable form of titanium dioxide and the major ore of titanium was discovered in 1803 by Werner in Spain, probably in Cajuelo, Burgos. Its name is derived from the Latin *rutilus*, red, in reference to the deep red color observed in some specimen when the transmitted light is viewed.

Brookite was named in honor of the English mineralogist, H.J. Brooke, and was discovered by A. Levy in 1825 at Snowen (Pays de Gales, England). Its crystals are dark brown to greenish black opaque.

Anatase, earlier called octahedrite, was named by R.J. Haüy in 1801 from the Greek word '*anatsis*' meaning 'extension', due to its longer vertical axis compared to that of rutile.

Table 3.1 Comparison of properties of anatase, brookite, and rutile.

Properties	Anatase	Brookite	Rutile
Crystal structure	Tetragonal	Orthorhombic	Tetragonal
Optical	Uniaxial, negative	Biaxial, positive	Uniaxial, negative
Density (kg/m ³)	3830	4240	4170
Unit cell	D _{4a} ¹⁹ .4TiO ₂	D _{2h} ¹⁵ .8TiO ₂	D _{4h} ¹² .3TiO ₂
Dimension (nm)			
A	0.3758	0.9166	0.4584
B	-	0.5436	-
C	0.9514	0.5135	2.953
Refractive index	2.490	-	2.903
Permittivity	31	-	114
Melting point	changes to rutile at high temp	-	1858 °C

For solar cell applications, the anatase structure is preferred over the rutile structure, as anatase exhibits a higher electron mobility, lower dielectric constant, lower density, and lower deposition temperature. The small differences in the Gibbs free energy (4–20 kJ/mole) between the three phases suggest that the metastable polymorphs are almost as stable as rutile at normal pressures and temperatures. If the particle sizes of the three crystalline phases are equal, anatase is most thermodynamically stable at sizes less than 11 nm, brookite is most stable between 11 and 35 nm, and rutile is most stable at sizes greater than 35 nm (Zhang and Banfield 2000).

The transformation from anatase to rutile is accompanied by the evolution of ca. 12.6 kJ/mol (3.01 kcal/mol), but the rate of transformation is greatly affected by temperature and by the presence of other substance which may either catalyze or inhibit the reaction. The lowest temperature at which conversion of anatase to rutile takes place at a measurable rate is ca. 700°C, but this is not a transition temperature. The change is not reversible; ΔG for the change from anatase to rutile is always negative.

Titanium (IV) oxide is thermally stable (mp 1855°C) and very resistant to chemical attack. When it is heated strongly under vacuum, there is a slight loss of oxygen corresponding to a change in composition to $\text{TiO}_{1.97}$. The product is dark blue but reverts to the original white color when it is heated in air.

3.2 Solvothermal method

These methods employ chemical reactions in aqueous (Yin et al. 2003) (hydrothermal method) or organic media (solvothermal method) such as methanol (Yin et al. 2003), 1,4 butanol, toluene (Kim et al. 2003a) under self-produced pressures at low temperatures (usually under 250 °C). Generally, but not always, a subsequent thermal treatment is required to crystallize the final material. The solvothermal treatment could be useful to control grain size, particle morphology,

crystalline phase, and surface chemistry by regulating the solution composition, reaction temperature, pressure, solvent properties, additives, and ageing time.

3.3 Quenching process

Quenching is a critical process that determines the final product of transformations of many materials. For the purposes of this proposal, it is defined as the mechanism of “rapid cooling” of metals. Quenching consists of cooling from a relatively high temperature to a fairly low temperature in a short period of time. The temperature differential and the rate of cooling may vary greatly, depending on the material being heated and on the required cooling rate. The temperature of the medium in which the article is then placed (quenched) may vary from that of ice water (0°C, or 32°F) to more than several hundreds of degrees Fahrenheit. Furthermore, the cooling power of the quenching medium may vary from as slow as that of still air to that of a violently agitated aqueous solution.

3.3.1 Classification of Quenching Methods and Techniques

These modifications have resulted in the arbitrary assignment of specific names to various quenching methods, such as direct quenching, fog quenching, and gas quenching.

3.3.1.1 Direct quenching refers to direct cooling (usually by a liquid quench) of the metal from its heat treating temperature to, or at least to near, ambient temperature.

3.3.1.2 Selective quenching is used when pre-selected areas of the workpiece must remain relatively unaffected by the quenching medium. This can be accomplished by insulating the area to be protected, or by allowing the quenchant to contact only those areas of the part that are to be quenched.

3.3.1.3 Time quenching is used when the cooling rate of the part being quenched must be changed abruptly at some time during the cooling cycle. The change in cooling rate may entail either an increase or a decrease in temperature, depending on which is needed to attain the desired results.

3.3.1.4 Spray quenching. With this method, streams of quenching liquid are directed at high pressure (up to 0.8 MPa, or 120 psi) to local areas of the workpiece. The cooling rate is rapid and uniform over the entire temperature range of the quenching cycle.

3.3.1.5 Fog quenching utilizes a fine fog or mist of liquid droplets and a gas carrier as cooling agents. This method of quenching, although similar to spray quenching, is less effective, because the quenching mist or fog is not readily adapted to rapid removal or replacement by cooler fog or mist once it has been heated by contact with the part being quenched.

3.3.1.6 Gas quenching. The term gas quenching includes cooling of metal parts in still or moving air, as well as in still or moving Inert gases, such as nitrogen or argon, and active gas mixtures such as protective atmospheres.

3.3.2 Quenching Media and Techniques

Many different media have been used for quenching. The most commonly used are included in the list below, including some that are used only to a very limited extent for specific applications:

- Water
- Brine solutions (aqueous)
- Caustic solutions (aqueous)
- Polymer solutions
- Oils
- Molten salts

- Molten metals
- Gases (still or moving)
- Fog quenching
- Dry dies (commonly water cooled, or cold slabs)

Only liquid quenching and gas quenching that concerns our work thus other quenching media will not mentioned in details. The details of liquid quenching and gas quenching are following

3.3.2.1 Water Quenching

Water was the original quenching medium used in commercial practice. Its other advantages are that it is inexpensive and readily available; it is easily disposed of without attendant problems of pollution or health hazard. Consequently, the quenching system can be extremely simple. One disadvantage of water as a quench is that its rapid cooling rate persists throughout the lower temperature range, in which distortion or cracking is like to occur. To reduce to temperature sensitivity of water, a wide variety of additives have been tried. The two most practical and effective additives are salt (sodium or calcium chloride and caustic (sodium or potassium hydroxide). Both of these materials increase the uniformity of the water quench without detracting from its cooling power. However these additives in themselves create certain drawback: including requirements for a closed system.

3.3.2.2 Gas Quenching

Gas quenching in its simplest form consists of removing a part from the furnace and allowing it to cool in still air; the only circulation is created by natural convection around the hot work piece. In gas quenching, the work piece is placed directly into the gas quenching zone or chamber, and heat is rapidly extracted from the metal by a fast-moving stream of gas. Various gases, ranging from air to complex mixtures, may be used for cooling, depending on process requirements.

In general, the quenching techniques in common use are:

- Immersion in a single quenchant (air or liquid) and cooling to near room temperature (usually slightly above) without interruption.

- Use of two quenching mediums on a timed basis, such as a partial quench in water, followed by oil; quench or quenching in molten salt, followed by finishing in air.

- Isothermal quenching, that is, predetermined temperature, then temperature until the phase completed.

- Spray quenching which usually uses an aqueous medium. This technique is most frequently used for quenching of induction- or flame-hardened parts, although it can be used for quenching of furnace- heated work pieces. Spray quenching offers the advantage of instantaneous control in timing as well as pressure regulation (Boyer 1988).

3.4 Defect structure of crystal material

Defects can be broadly divided into two groups: stoichiometric defects in which the crystal composition is unchanged on introducing the defects and non-stoichiometric defects, which are a consequence of a change in crystal composition. It is well-known that the surface reactivity is not the same when the surface is regular (stoichiometric) or reduced (substoichiometric) (Calatayud et al. 2004). These defects affect the chemical properties of solids in very significant ways, and play a key role in controlling the rate at which solids react. As a general rule, the most favorable adsorption modes on a perfect surface preserve the electronic gap of the oxide and can be understood in terms of acid-base reaction mechanisms; on the contrary, the adsorption on a reduced surface implies a redox mechanism in order to restore the gap that is decreased or has disappeared by effect of them reduction. Two such defects particular importance is the Frenkel and Schottky defects. Only point defect that

concerns our work thus large-scale imperfections will not mentioned in details. The details of point defects are following

3.4.1 Vacancies: Schottky defects

Consider the simplest crystal defect, namely that of an atomic site becoming vacant, with the missing atom migrating to the crystal surface. This process will be energetically unfavorable, costing the system a change in energy. The defects arising from balanced populations of cation and anion vacancies are now known as Schottky defects.

Schottky defects are frequently represented in Figure 3.2. This represents a Schottky defect in a crystal structure of the sodium chloride type, the projection shown in this diagram representing a (100) plane. In this case, Schottky defect will consist of the appropriate numbers of cation and anion vacancies to form an electrically neutral total.

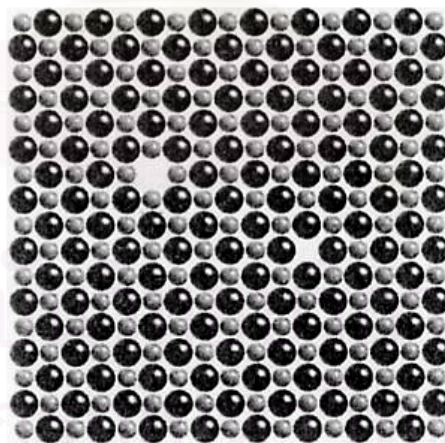


Figure 3.2 Cation and anion charge-balanced Schottky defects in NaCl. The metal atoms are smaller than the non-metal atoms. The defect consists of vacancies on both metal and non-metal sites

3.4.2 Interstitial defects: Frenkel defects

In crystals that not pack with high efficiency, it is possible for atoms to occupy sites that are normally vacant, called interstitial sites. The Frenkel defect contains interstitial-vacancy pairs, formed as a result of the transfer of atoms or ions into interstitial sites, leaving vacancies behind at the regular sites. This process is illustrated in Figure 3.3.

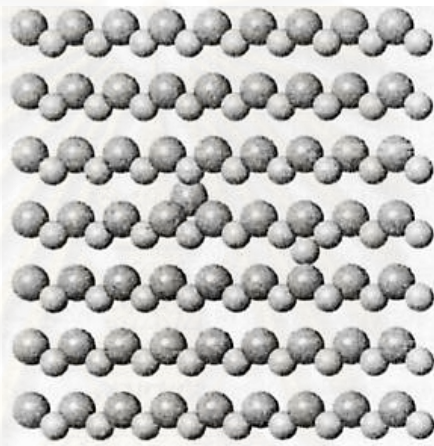


Figure 3.3 Pair of charge-balanced Frenkel defects in AgI. The metal atoms are smaller than the non-metal atoms. The defects consist of equal numbers of vacancies on either the metal or non-metal or non-metal sub-lattice and interstitial ions of the same type

3.5 Photocatalytic reaction

Unlike metals, which have a continuum of electronic states, semiconductors exhibit a void energy region in which no energy levels are available to promote the recombination of an electron and hole produced by photoactivation in the solid. The void region that extends from the top of the filled valence band to the bottom of the vacant conduction band is called the band gap (Linsebigler et al. 1995).

Absorption of a photon by semiconducting solids excites an electron (e^-) from the valence band to the conduction band if the photon energy, $h\nu$, equals or exceeds

the band gap of the semiconductor/photocatalyst. Simultaneously, an electron vacancy or a positive charge called a hole (h^+) is also generated in the valence band (Figure 3.4). Ultraviolet (UV) or near-ultraviolet photons are typically required for this kind of reaction.

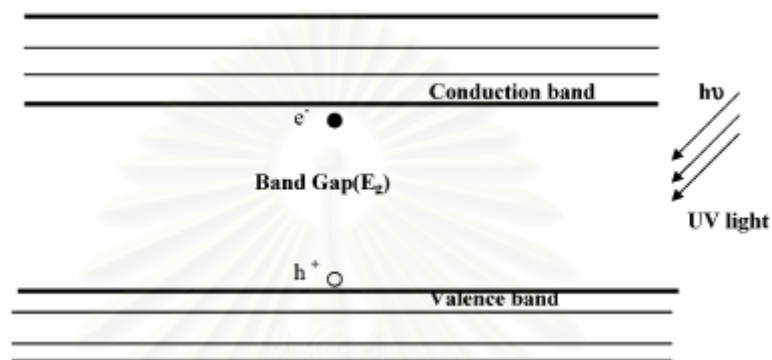


Figure 3.4 Band-gap diagram (formation of holes (h^+) and electrons (e^-) upon UV irradiation of semiconductor surface)

The electron-hole pair (e^-h^+ pair) thus created migrates to the photocatalyst surface where it either recombines, producing thermal energy, or participates in redox reactions with the compounds adsorbed on the photocatalyst (see Figure 3.5). The lifetime of an e^-h^+ pair is a few nanoseconds, but this is still long enough for promoting redox reactions in the solution or gas phase in contact with the semiconductor.

Generally, the hole oxidizes water to hydroxyl radicals (which subsequently initiate a chain of reactions leading to the oxidation of organics), or it can be combined with the electron from a donor species (D), depending on the mechanism of the photoreaction. Similarly, the electron can be donated to an electron acceptor (A) such as an oxygen molecule (leading to formation of superoxide radical) or a metal ion (with a redox potential more positive than the band gap of the photocatalyst). This metal ion can be reduced to its lower valence states and deposited on the surface of the catalyst. The electron-transfer process is more efficient if the species are preadsorbed on the surface (Linsebigler et al. 1995).

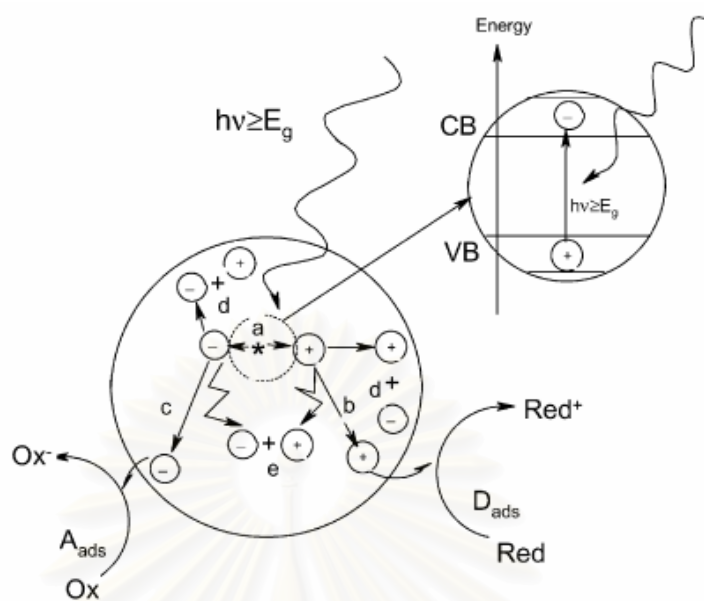
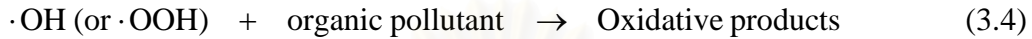
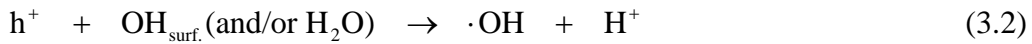
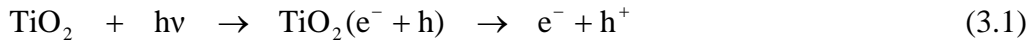


Figure 3.5 Main processes occurring on a semiconductor particle: (a) electron–hole generation; (b) oxidation of donor (D); (c) reduction of acceptor (A); (d) and (e) electron–hole recombination at surface and in bulk, respectively

The detailed mechanism of the photocatalytic process on the TiO_2 surface is still not completely clear, particularly that concerning the initial steps involved in the reaction of reactive oxygen species and organic molecules. Past experience has shown that TiO_2 particles absorb UV light of energy greater than bandgap (ca. 3.1 eV for P-25, ca. 3.2 eV for pure anatase, and ca. 3.0 eV for pure rutile as deduced from diffuse reflectance spectroscopy) to generate electron/ hole pairs (Eq. (1)). Subsequent to various steps, the holes (h^+) are ultimately trapped by surface HO^- groups (or H_2O) at the particle surface to yield $\bullet OH$ radicals (and H^+ ; Eq. (2)). Dissolved oxygen molecules react with conduction band electrons (e^-) to yield superoxide radical anions, $O_2^{\bullet -}$, which on protonation generate the hydroperoxy, $\bullet OOH$, radicals (Eq. (2)). An important factor for the efficient photooxidation of organic substrates then with UV/ TiO_2 -driven photocatalysis will depend on the concentration of $\bullet OH$ radicals by photooxidation of surface hydroxyl groups and/or chemisorbed H_2O (Horikoshi et al. 2003).



The ability of a semiconductor to undergo photoinduced electron transfer to adsorbed species on its surface is governed by the band energy positions of the semiconductor and the redox potentials of the adsorbate. In Figure 3.6, in terms of energy usage, the complete electrolytic decomposition of water is possible if the energy of the conduction band is at least as negative (i.e., higher in the diagram) as that required to reduce water to oxygen gas (0.0 V in acid solution), and the VB is at least as positive (i.e., lower) as that required to oxidize water to oxygen gas (+1.23 V). The complete decomposition of water is thus theoretically possible if a semiconductor that has the minimum band gap energy of 1.23 eV is illuminated with light, assuming that the energies of valence band and conduction band are located at appropriate positions. All of the semiconductors with small band gaps, however, have a strong tendency to decompose and dissolve when illuminated in aqueous solution.

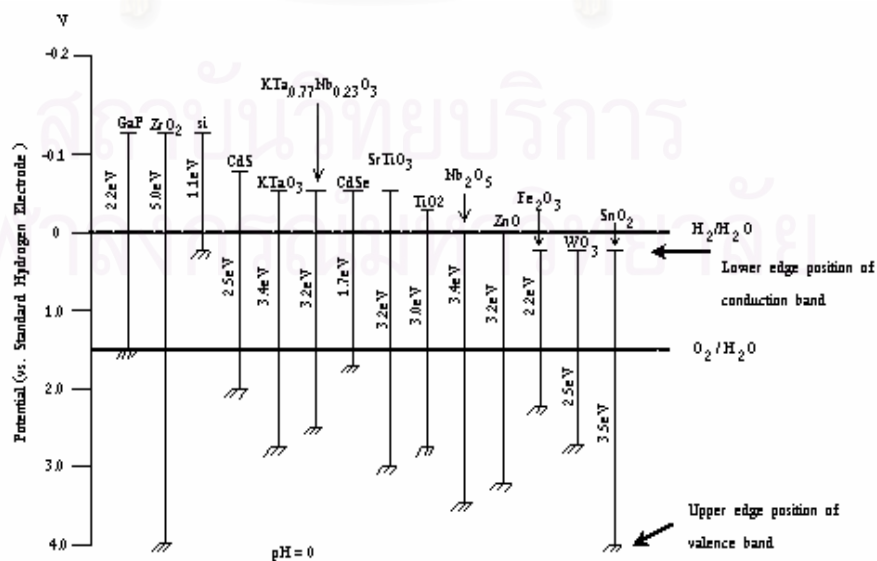


Figure 3.6 Energy diagram for typical semiconductors

3.6 Mechanisms of semiconductor photocatalytic water-splitting or hydrogen production

The electronic structure of a semiconductor plays a key role in semiconductor photocatalysis. Unlike a conductor, a semiconductor consists of VB and CB. Energy difference between these two levels is said to be the band gap (E_g). Without excitation, both the electrons and holes are in valence band. When semiconductors are excited by photons with energy equal to or higher than their band gap energy level, electrons receive energy from the photons and are thus promoted from VB to CB if the energy gain is higher than the band gap energy level. For semiconductor titanium dioxide, the reaction is expressed as:



The photo-generated electrons and holes can recombine in bulk or on surface of the semiconductor within a very short time, releasing energy in the form of heat or photons. Electrons and holes that migrate to the surface of the semiconductor without recombination can, respectively, reduce and oxidize the reactants adsorbed by the semiconductor. The reduction and oxidation reactions are the basic mechanisms of photocatalytic hydrogen production and photocatalytic water/air purification, respectively. Both surface adsorption as well as photocatalytic reactions can be enhanced by nano-sized semiconductors as more reactive surface area is available.

For hydrogen production, the CB level should be more negative than hydrogen production level ($E_{\text{H}_2/\text{H}_2\text{O}}$) while the VB should be more positive than water oxidation level ($E_{\text{O}_2/\text{H}_2\text{O}}$) for efficient oxygen production from water by photocatalysis.

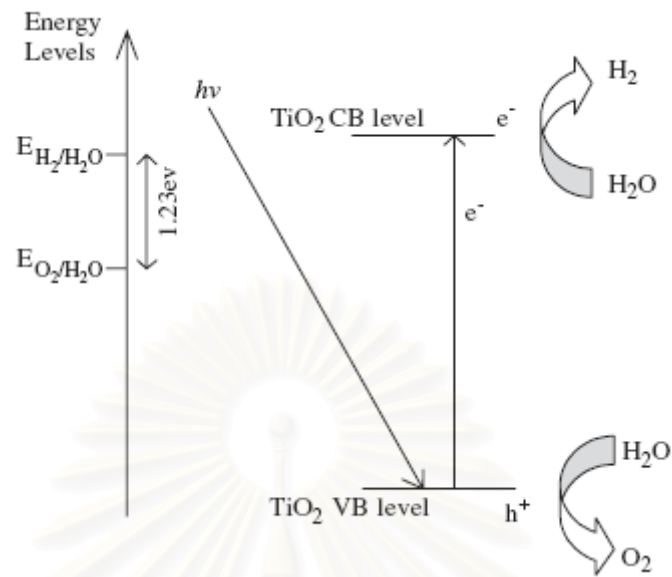


Figure 3.7 Mechanism of TiO_2 photocatalytic water splitting for hydrogen production (Meng Ni 2005)

The photocatalytic hydrogen production by titanium dioxide is shown in Figure 3.7. Theoretically, all types of semiconductors that satisfy the above-mentioned requirements can be used as photocatalysts for hydrogen production. However, most of the semiconductors, such as CdS and SiC, that cause photocorrosion, are not suitable for water-splitting. Having strong catalytic activity, high chemical stability and long lifetime of electron/hole pairs, titanium dioxide is the most widely used photocatalyst. Presently, the energy conversion efficiency from solar to hydrogen by titanium dioxide photocatalytic water-splitting is still low, mainly due to the following reasons:

(1) Recombination of photo-generated electron/hole pairs: CB electrons can recombine with VB holes very quickly and release energy in the form of unproductive heat or photons;

(2) Fast backward reaction: Decomposition of water into hydrogen and oxygen is an energy increasing process, thus backward reaction (recombination of hydrogen and oxygen into water) easily proceeds;

(3) Inability to utilize visible light: The band gap of titanium dioxide is about 3.2 eV and only UV light can be utilized for hydrogen production. Since the UV light only accounts for about 4% of the solar radiation energy while the visible light contributes about 50%, the inability to utilize visible light limits the efficiency of solar photocatalytic hydrogen production (Meng Ni 2005).



สถาบันวิทยบริการ
จุฬาลงกรณ์มหาวิทยาลัย

CHAPTER IV

EXPERIMENTS

The synthesis of titanium (IV) oxide using solvothermal process in organic solvent is explained in this chapter. The chemicals, sample preparation and characterization are also explained.

4.1 Chemicals

The details of chemicals for preparation of titanium dioxide catalyst, titanium dioxide synthesized by solvothermal method, and this titanium dioxide quenched in various quenching media, and used in photocatalytic decomposition of water to hydrogen were shown in Table 4.1

Table 4.1 Chemical used in the experiment

Chemical	supplier
Titanium (IV) tert-butoxide (97% TNB, $\text{Ti}[\text{O}(\text{CH}_2)_3\text{CH}_3]_4$)	Aldrich
Toluene (99.999%, $\text{C}_6\text{H}_5\text{CH}_3$)	Fisher Scientific
Hydrogen peroxide (30%, H_2O_2)	Merck
Methyl alcohol (99.9%, CH_3OH)	Merck

4.2 Equipment

4.2.1 Autoclave reactor

The detailed schematic diagram of the equipment used for titanium dioxide synthesis is mainly consisted of an autoclave reactor, as shown in Figure 4.1. The autoclave reactor is shown in Figure 4.2. The reactor has the following features.

- Made from stainless steel
- Volume of 1000 cm³
- 10 cm inside diameter
- Maximum temperature of 350 °C
- Pressure gauge in the range of 0 – 140 bar
- Relief valve used to prevent runaway reaction
- Iron jacket was used to reduce the volume of autoclave to be 300 cm³
- Test tube was used to contain the reagent and glycol

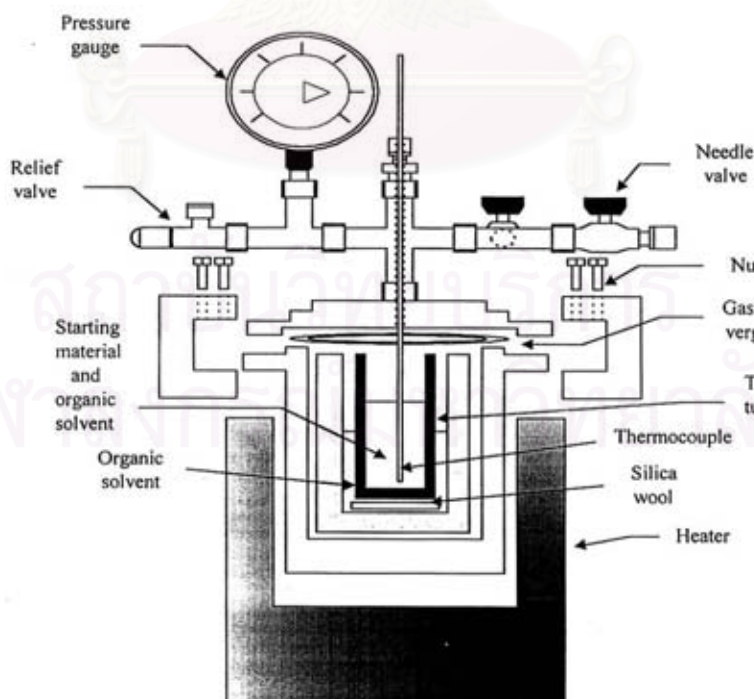


Figure 4.1 Autoclave reactor

4.2.2 Temperature program controller

A temperature program controller CHINO DB1000F was connected to a thermocouple with a 0.5 mm diameter located the autoclave.

4.2.3 Electrical furnace (Heater)

Electrical furnace was used to supply the required heat to the autoclave for the reaction.

4.2.4 Gas controlling system

Nitrogen was set with a pressure regulator (0 – 150 bar) and needle valves are used to release gas from autoclave.

The diagram of the reaction equipment is shown in Figure 4.2

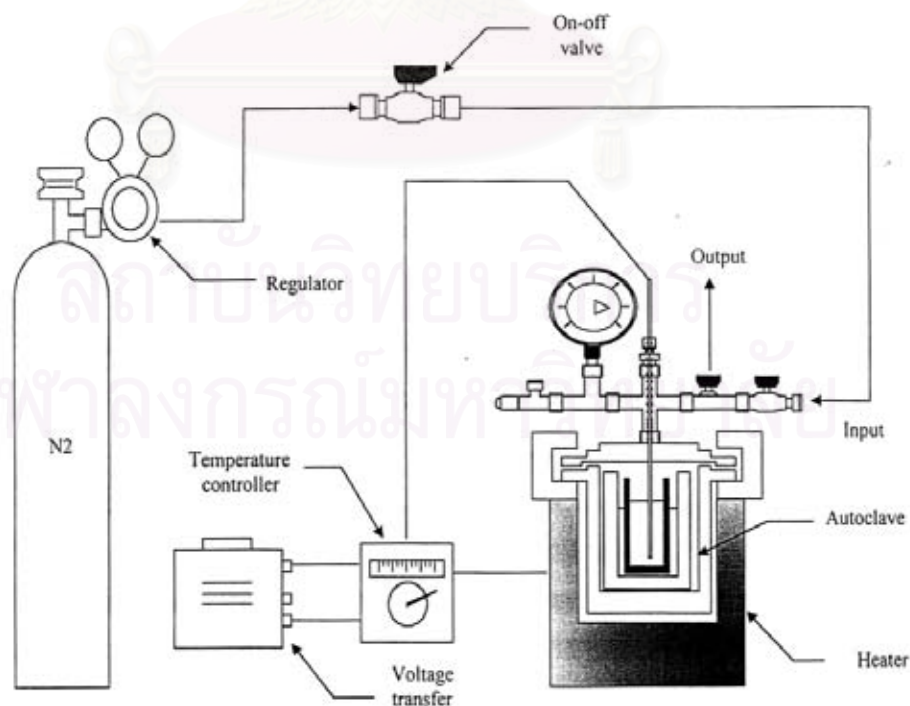


Figure 4.2 Diagram of the reaction equipment for the catalyst preparation

4.3 Catalyst Preparation

4.3.1 Preparation of Titanium dioxide nanoparticles

Nanocrystalline titanium dioxide was prepared using the solvothermal method in the same manner as that of (Payakgul et al. 2005). Titanium (IV) n-butoxide (purity 97 %, Aldrich) was used as the starting material. Approximately 25 g of titanium n-butoxide was suspended in 100 ml of toluene, in a test tube, which was then placed in a 300 ml autoclave. In the case of preparation modified titanium dioxide, a desired amount of the second metal precursor will be added into the test tube. The same solvent was filled in the gap between the test tube and the autoclave wall. The autoclave was purged completely by nitrogen after that it was heated up to the desired temperature at 573 K with the rate of 2.5 K/min. The temperature of the autoclave was held constant at 573 K for 2 h and then cooled down to room temperature. The obtained titanium dioxide was washed by methanol for several times and finally dried in air.

The synthesis product was then calcined in a box furnace by heating up to the desired temperature, in the range of 563–583 K, at a rate of 10 K/min and held at that temperature for 1 h in order to remove any impurity that might remain on the samples after washing with methanol.

4.3.2 Modified Titanium dioxide nanoparticles

For quenching pre-treatment, the synthesized titanium dioxide was dried in air atmosphere at 573 K with a heating rate of 10 K/min for 1 h and then it was taken out and immediately quenched in various quenching media. In this study, both liquid phase and gas phase media were used.

4.3.2.1 For quenching in gas phase media, air at 77 K, room temperature and 373 K (sample A, B and C) were selected.

4.3.2.2 For quenching in liquid phase media, 30% wt hydrogen peroxide at room temperature and 373 K (sample D and E), water at room temperature and 373 K (sample F and G), were selected.

After the samples were quenched in the media for 30 min, all samples were dried in air at room temperature and stored in the desiccator.

4.4 Photocatalytic Activity Evaluations

The effect of quenching process on photocatalytic activity of titanium dioxide powder was performed by using photocatalytic decomposition of water to hydrogen as a model reaction in Figure 4.3.

The photocatalytic activity was performed over 0.3 g of titanium dioxide catalyst was suspended in water/methanol solution in the 125 mL vertical tubular batch reactor made of Pyrex, and the reactor was half-filled with a water/ methanol solution volume ratio is 4 : 1, and methanol was added as the sacrificial reagent. Ultra high purity argon manufactured by Thai Industrial Gas Limited (TIG) was used for purge in reactor for 10 min for exhausting gases inside the reactor.

Titanium dioxide photocatalyst was suspended by magnetic stirrer and irradiated with 4 UV-light tubes, each having a power of 15 W. The unfilled space above the solution was evacuated at the beginning of reaction, and the rate of evolution of hydrogen was determined from gas phase products by gas chromatography (Shimadzu GC-8A (TCD), molecular sieve 5-Å column, Ar carrier). The operating conditions for each instrument are shown in the Table 4.2.

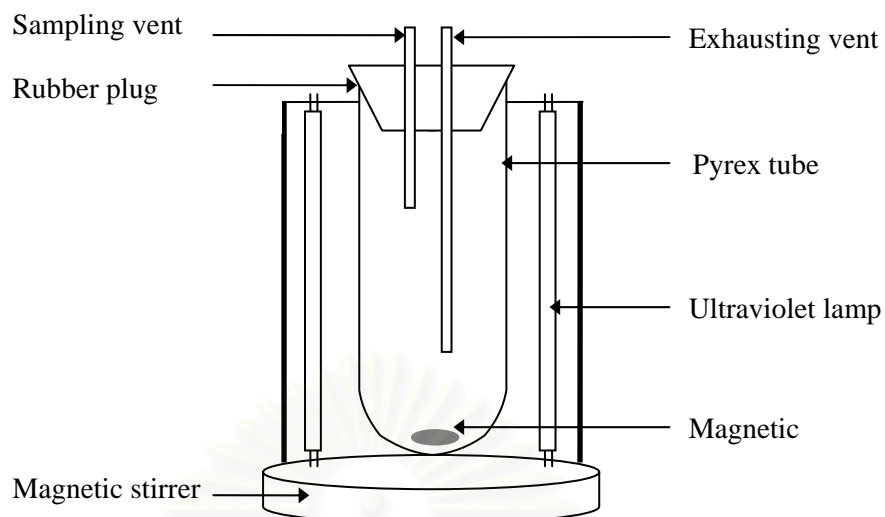


Figure 4.3 Experiment set-up of photochemical reactor.

Table 4.2 Operating condition for gas chromatograph

Gas Chromatograph	SHIMADZU GC-8A
Detector	TCD
Column	Molecular sieve 5A
- Column material	SUS
- Length	2 m
- Outer diameter	4 mm
- Inner diameter	3 mm
- Mesh range	60/80
- Maximum temperature	350 °C
Carrier gas	Ar (99.999%)
Carrier gas flow (ml/min)	30 cc/min
Column temperature	
- initial (°C)	60
- final (°C)	60
Injector temperature (°C)	100
Detector temperature (°C)	100
Current (mA)	70
Analyzed gas	Hydrogen

4.5 Catalyst Characterization

The obtained products were characterized by using various techniques, as following:

4.5.1 X-ray diffraction analysis (XRD)

The XRD spectra were measured by using a SIEMENS D5000 X-ray diffractometer using Cu K α radiation with a Ni filter. The crystallite size of titanium dioxide was determined from half-height width of the 101 diffraction peak of anatase using the Sherrer equation. The condition of the measurement is show as followed:

2 θ range of detection	:	20 - 80°
Resolution	:	0.02°
Number of scan	:	10

4.5.2 Surface area measurement

The specific surface area of titanium dioxide was measured according to the single point BET method (Brunauer Emmett Teller), by using nitrogen as the adsorbate. The operating conditions are as follows:

Sample weight	:	~ 0.2 g
Degas temperature	:	200 °C for as-synthesized sample

4.5.3 Temperature programmed desorption (TPD)

Temperature programmed desorption using CO $_2$ as a probe molecule (CO $_2$ -TPD) was performed to determine the Ti $^{3+}$ site on surface titanium dioxide. It was carried out using 0.05 g of a titanium dioxide sample. Titanium dioxide was dosed by 1% CO $_2$ in He for 1 h in liquid nitrogen and then desorped in a range of temperature from 123 to 253 K by level controlling. A Gow-Mac (Series 150 thermal conductivity

detector) gas chromatography equipped with a thermal conductivity detector was used to analyze CO₂.

4.5.4 Electron spin resonance spectroscopy (ESR)

Electron spin resonance spectroscopy was conducted in vacuum at room temperature using JEOL, JES-RE2X electron spin resonance spectrometer. It was performed to monitor the surface defect (Ti³⁺) on surface titanium dioxide. Recorded spectra were scanned and were converted to a g-value scale referring to a Mn²⁺ marker.

4.5.5 UV-visible absorption spectroscopy (UV-Vis)

To study the light reflectance behavior of the catalysts, the diffuse reflectance spectra of the titanium dioxide catalyst in the wavelength range of 280-500 nm were obtained using a UV- visible scanning spectrophotometer (Perkin Elmer Lambda 650, λ between 280-500 nm and step size 1 nm), while BaSO₄ was used as reference.

4.5.6 Thermal gravimetric Analysis (TGA)

The free carbon, residual carbon content and thermal behaviors of the samples were determined by using TG/DTA analysis on a Diamond TG/DTA thermogravimetric instrument. The analysis was performed from temperature of 25 to 700 °C under a heating rate of 10 °C/min in 100 ml/min flow of oxygen.

4.5.7 Fourier-Transform Infrared Spectroscopy (FT-IR)

The functional groups on the catalyst surface were determined using infrared spectroscopy. The equipment used was a Nicolet Impact 400 infrared spectrometer. IR spectra were recorded from an accumulation of 64 scans in 4000-400 cm⁻¹ range with a resolution of 2 cm⁻¹.

CHAPTER V

RESULTS AND DISCUSSION

The study in order to investigate the quenching process of titanium dioxide prepared in laboratory by solvothermal method. The catalytic activity was evaluated using the photocatalytic water decomposition to hydrogen. The results in this chapter are divided into three major parts. The first part describes the formation of titanium dioxide synthesized by solvothermal method (section 5.1), the characteristics of structure and surface properties of TiO₂ quenched in different media titanium dioxide (section 5.2), effect of quenching process on surface defect of TiO₂ (section 5.3), photocatalytic activity of the TiO₂ quenched in various media (section 5.4) and the last part describes the photocatalytic reaction (section 5.5).

5.1 Formation of Titanium Dioxide

Titanium dioxide was also synthesized in toluene at 300 °C for 2 h, thermal decomposition of titanium (IV) tert-butoxide (TNB) in toluene occurred under inert organic solvent condition, yielding a ≡Ti-O⁻ anion. The nucleophilic attack of the titanate ion on another ion and crystallization was taken place, finally yielding the anatase titanium dioxide (Theinkeaw 2000). The mechanism of TNB in toluene can be depicted as shown in Figure 5.1.

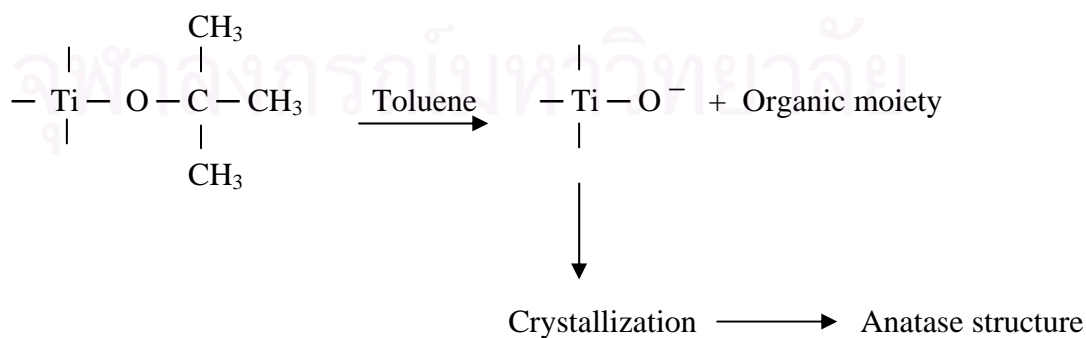


Figure 5.1 Mechanism of reaction in toluene for the titanium dioxide (Theinkeaw 2000)

5.2 Structure and surface properties of TiO₂ quenched in different media

5.2.1 X-ray diffraction analysis (XRD)

Titanium dioxide (TiO₂) powders were synthesized by solvothermal method using titanium butoxide as the precursor. In order to modify their surface properties, the titanium dioxide powders were subjected to quenching processes using various media and quenching conditions. Air, 30%wt hydrogen peroxide and water at different temperatures are chosen as the quenching media for this study. The phase identification of titanium dioxide is based on the results from X-ray diffraction. The XRD pattern of titanium dioxide samples quenched in various quenching media and quenching conditions in the 2θ ranges from 20° to 80° is shown in Figure 5.2. The XRD spectra of the titanium dioxide exhibited strong diffraction peaks at 26°, 37°, 48°, 55°, 56°, 62°, 69°, 71°, and 75° 2θ indicating titanium dioxide in the anatase phase (Suriye et al. 2007). All of those peaks can be attributed to titanium dioxide anatase phase. Thus, nanocrystalline pure anatase titanium dioxide can be produced by the solvothermal method without any contamination of other phases.

The crystallite size of titanium dioxide sample was determined from the half-height width of the 101 diffraction peak of anatase titanium dioxide using Sherrer's equation. The crystallite size of the titanium dioxide was found to be ca. 10 nm.

From the XRD results, the titanium dioxide samples had similar crystallinity shown by the same ordering in the structure of the titanium dioxide particles with the same intensity of the XRD peaks. Thus indicating, quenching process of the modification titanium dioxide is not influence to crystallite sizes and phase of titanium dioxide.

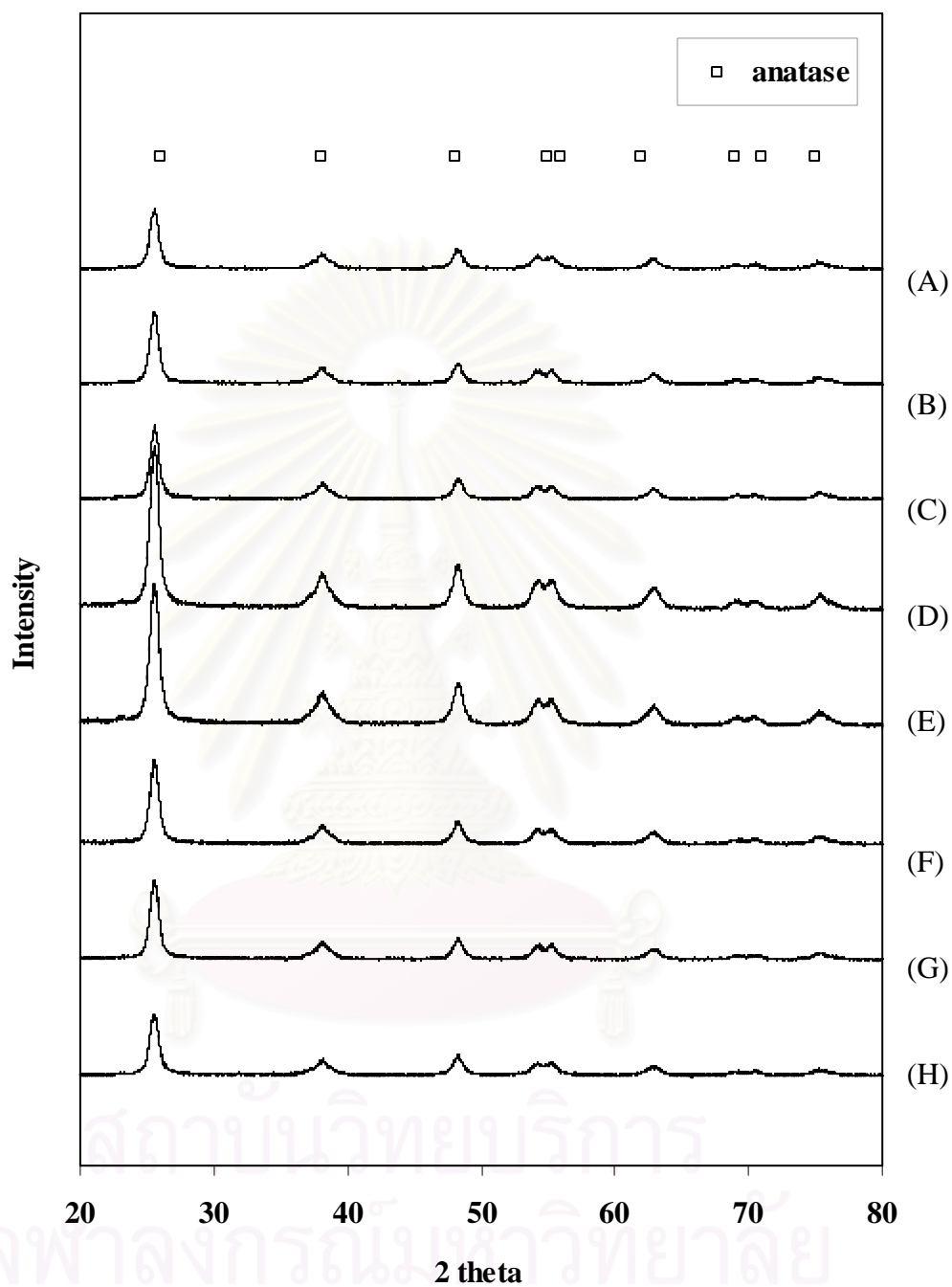


Figure 5.2 The XRD patterns of the TiO₂ obtained from quenching in various media; (A) Air at 77 K, (B) Air at RT, (C) Air at 373 K, (D) 30% wt H₂O₂ at RT, (E) 30% wt H₂O₂ at 373 K, (F) H₂O at RT, (G) H₂O at 373 K and (H) TiO₂

5.2.2 Surface area measurement

The specific surface area of titanium dioxide samples quenched in various quenching media and quenching conditions were measured according to the Brunauer Emmett Teller (BET) surface area, by using nitrogen as the adsorption at 77 K in a Micromeritics Chemisorb 2750 automated system. All the samples were dried at 200 °C for 1 h in a 30% N₂-helium flow prior to BET measurements. The measured BET surface areas of titanium dioxide samples were in the range of 80-94 m²/g. There were not significantly differences in BET surface area of titanium dioxide quenched in various quenching media. The BET surface area of titanium dioxide prepared in this study is shown in Table 5.1.

The crystallites size and BET surface area of titanium dioxide prepared in this study are shown in Table 5.1.

Table 5.1 The crystallite size and BET surface area of titanium dioxide

Samples	Quenching media	Crystallite size (nm)	BET surface area (m ² /g)
A	Air at 77 K	10.3	92.4
B	Air at RT	10.5	91.3
C	Air at 373 K	10.9	88.2
D	30% wt H ₂ O ₂ at RT	9.9	88.8
E	30% wt H ₂ O ₂ at 373 K	9.7	94.2
F	H ₂ O at RT	10.3	92.3
G	H ₂ O at 373 K	10.0	85.5
H (TiO ₂)	-	10.2	80.9

5.2.3 The characteristics of surface adsorption site of TiO₂ samples

Typically, quenching treatment of metal can generate nucleation of dislocations, surface defect and concentration of stress on the surface (Thompson et al. 2003). Defect sites on TiO₂ photocatalysts are known as active sites (Diebold 2003), electronic promoters (Ramirez et al. 1999), or electron traps thus modification of TiO₂ surface is an alternative way to improve their photocatalytic activities by enhancing the amount of defect sites.

The characteristics of surface adsorption sites of the TiO₂ samples were studied by means of temperature program desorption of CO₂ from 100-310 K. The results are shown in Figure 5.3. All of the TiO₂ samples exhibited two main desorption peaks at 170 K and 200 K which could be attributed to adsorption of CO₂ on two different structures of TiO₂ surface as reported by Tracy et al. (Nakaoka and Nosaka 1997). The peak at ca. 170 K is attributed to CO₂ molecules bounding to regular five-coordinate Ti⁴⁺ site which was considered as the perfected titania structure. The second peak at ca. 200 K has been considered as desorption of CO₂ molecules bounding to Ti³⁺ defect sites of titanium dioxide. From the CO₂-TPD results, it was observed that the CO₂ desorption peak areas at ca. 200 K of the TiO₂ samples apparently increased in the order: air at 77 K > air at RT > air at 373 K > 30% wt H₂O₂ at RT > 30% wt H₂O₂ at 373 K > H₂O at RT > H₂O at 373 K.

The results in Figure 5.4 and Table 5.2 were shown the ratios of peak areas of Ti³⁺/Ti⁴⁺ and various quenching media were also determined from the CO₂-TPD measurement. It was found to the amount of Ti³⁺ surface defects increased in the order: air at 77 K > air at RT > air at 373 K > 30% wt H₂O₂ at RT > 30% wt H₂O₂ at 373 K > H₂O at RT > H₂O at 373 K.

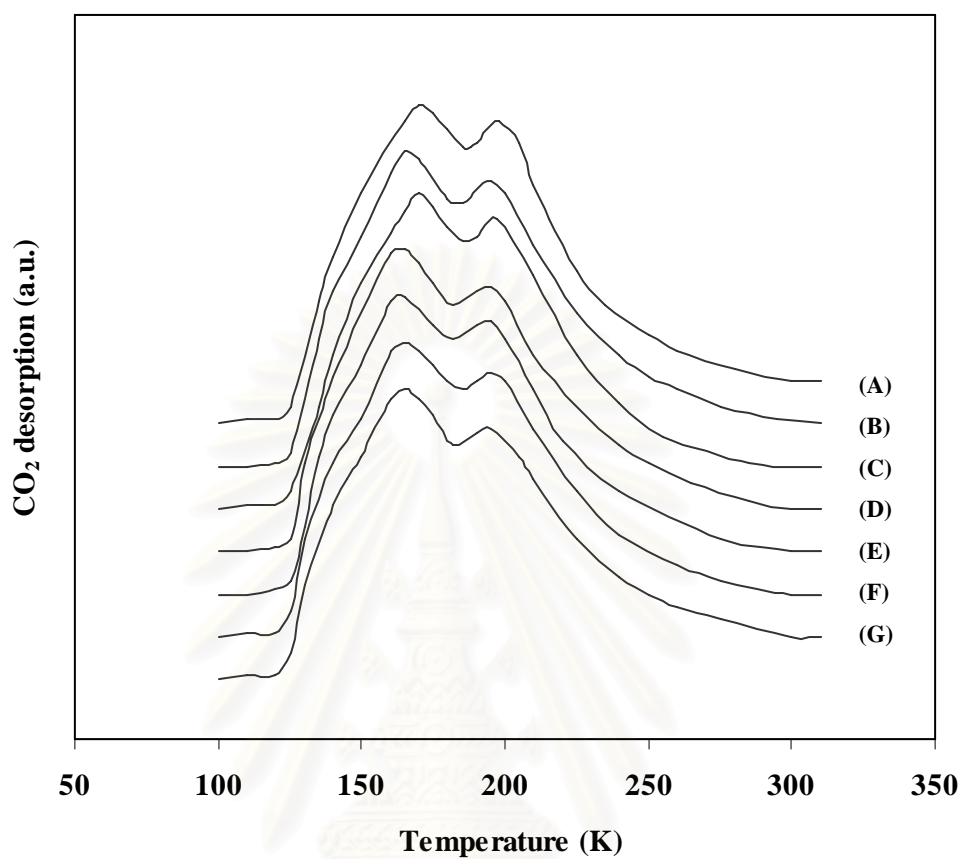


Figure 5.3 Thermal desorption spectra for CO₂ adsorbed on TiO₂ quenched in different media; (A) Air at 77 K, (B) Air at RT, (C) Air at 373 K, (D) 30% wt H₂O₂ at RT, (E) 30%wt H₂O₂ at 373 K, (F) H₂O at RT and (G) H₂O at 373 K

สถาบันวิทยบริการ
จุฬาลงกรณ์มหาวิทยาลัย

Table 5.2 Ratios of peak areas of Ti^{3+}/Ti^{4+} were also determined from the temperature program desorption (CO_2 -TPD)

Samples	Quenching media	Ratio of peak areas of Ti^{3+}/Ti^{4+}
A	Air at 77 K	0.2479
B	Air at RT	0.2330
C	Air at 373 K	0.2225
D	30% wt H_2O_2 at RT	0.2201
E	30% wt H_2O_2 at 373 K	0.2173
F	H_2O at RT	0.2103
G	H_2O at 373 K	0.2005

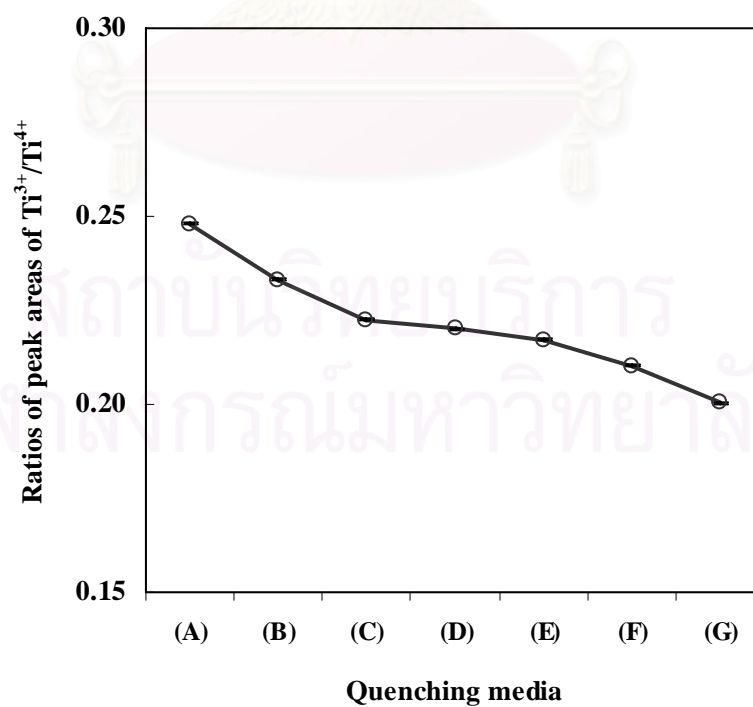


Figure 5.4 Ratios of peak areas of Ti^{3+}/Ti^{4+} and various quenching media

5.2.4 Electron spin resonance spectroscopy (ESR)

Figure 5.5 displays the results obtained from ESR measurements at room temperature for TiO_2 quenched in various media at different temperature, comparing the amount of Ti^{3+} defects on the TiO_2 . The peak observed was assigned to Ti^{3+} surface defects. The results in Figure 5.6 shown the TiO_2 samples apparently increased in the order: air at 77 K > air at RT > air at 373 K > 30% wt H_2O_2 at RT > 30% wt H_2O_2 at 373 K > H_2O at RT > H_2O at 373 K, the Ti^{3+} peak became higher and thus the amount of Ti^{3+} surface defects increased. The data of the amount of Ti^{3+} surface defects was given in the Table 5.3.

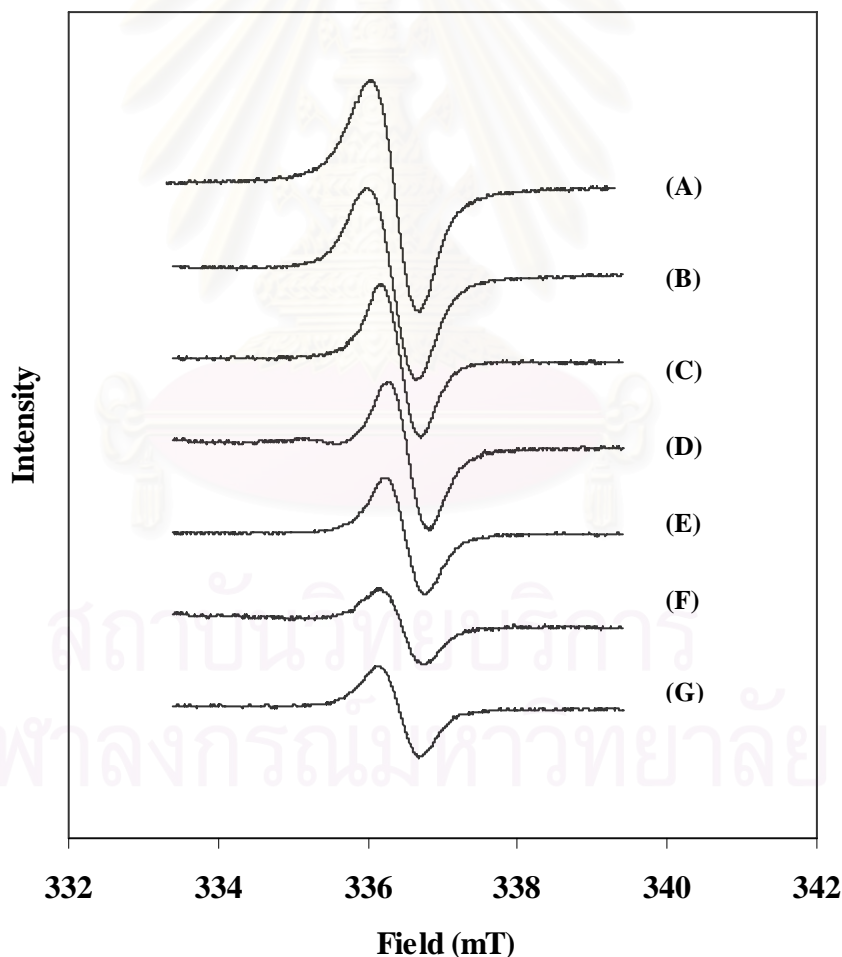


Figure 5.5 ESR spectra of TiO_2 quenched in different media; (A) Air at 77 K, (B) Air at RT, (C) Air at 373 K, (D) 30% wt H_2O_2 at RT, (E) 30%wt H_2O_2 at 373 K, (F) H_2O at RT and (G) H_2O at 373 K

Table 5.3 The amount of Ti^{3+} surface defect of TiO_2 were also determined from the ESR measurements

Samples	Quenching media	BET surface area (m^2/g)	Weight (g)	Intensity of Ti^{3+} surface defects per surface area
A	Air at 77 K	92.4	0.081	356.7
B	Air at RT	91.3	0.080	301.9
C	Air at 373 K	88.2	0.081	247.4
D	30% wt H_2O_2 at RT	88.8	0.079	241.9
E	30% wt H_2O_2 at 373 K	94.2	0.080	179.5
F	H_2O at RT	92.3	0.081	141.4
G	H_2O at 373 K	85.5	0.080	128.7

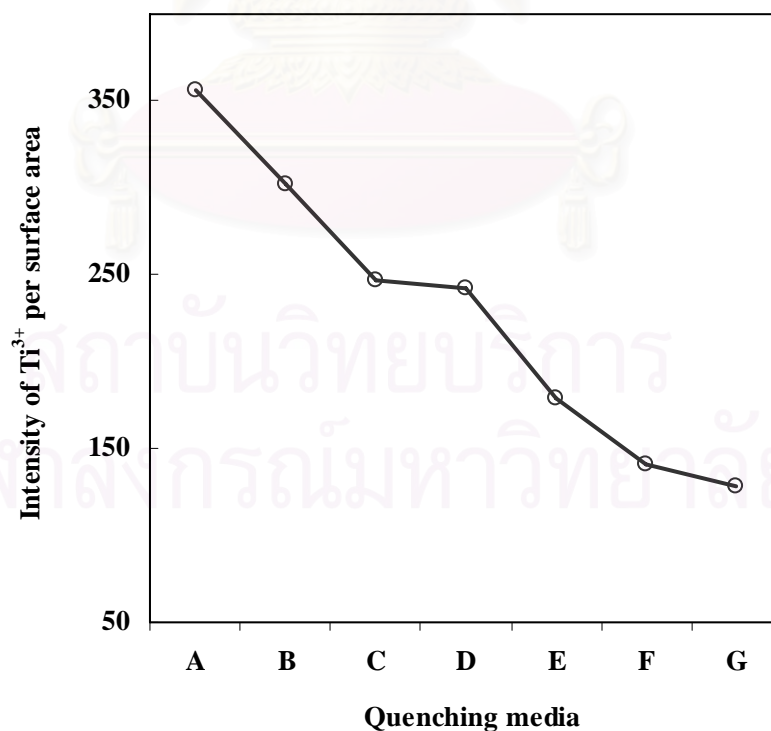


Figure 5.6 Intensity of Ti^{3+} surface defects per surface area and various quenching media

5.3 Effect of quenching process on surface defect of TiO₂

5.3.1 Effect of temperature for the quenching media on surface defect

From the CO₂-TPD results in this study, however, emphasize the influence of quenching condition (temperature) and medium on photocatalytic activity of TiO₂. It is revealed that selected quenching pre-treatment processes can modify the surface properties of TiO₂. In other words, temperature of the quenching media has a significant impact on the amount of Ti³⁺ surface defects on the TiO₂. Considering the TiO₂ samples quenched in the same type of quenching media (i.e., in Air, 30% wt H₂O₂ and H₂O), it was found that TiO₂ samples quenched in cooler media exhibited higher amount of Ti³⁺ surface defect than those quenched in hotter ones.

The results in Figure 5.7 5.8 and 5.9 were shown the thermal desorption spectra for CO₂ adsorbed on TiO₂ quenched in various media at different temperature, comparing the amount of Ti³⁺ surface defects on the TiO₂ quenched in different temperature of the quenching media in air water and 30% wt hydrogen peroxide at different temperature respectively, it observed TiO₂ quenched in air at 77 K showed much higher amount of Ti³⁺ surface defects than the one quenched in air at room temperature and air at 373 K, respectively. In other words, TiO₂ quenched in water at room temperature showed much higher amount of Ti³⁺ surface defects than the one quenched at 373 K. These results can probably be explained in terms of the thermal shock effect. The large difference in temperature between media and TiO₂ surface may lead to modification of the surface properties by increasing the amount of Ti³⁺ surface defects on the TiO₂ surface.

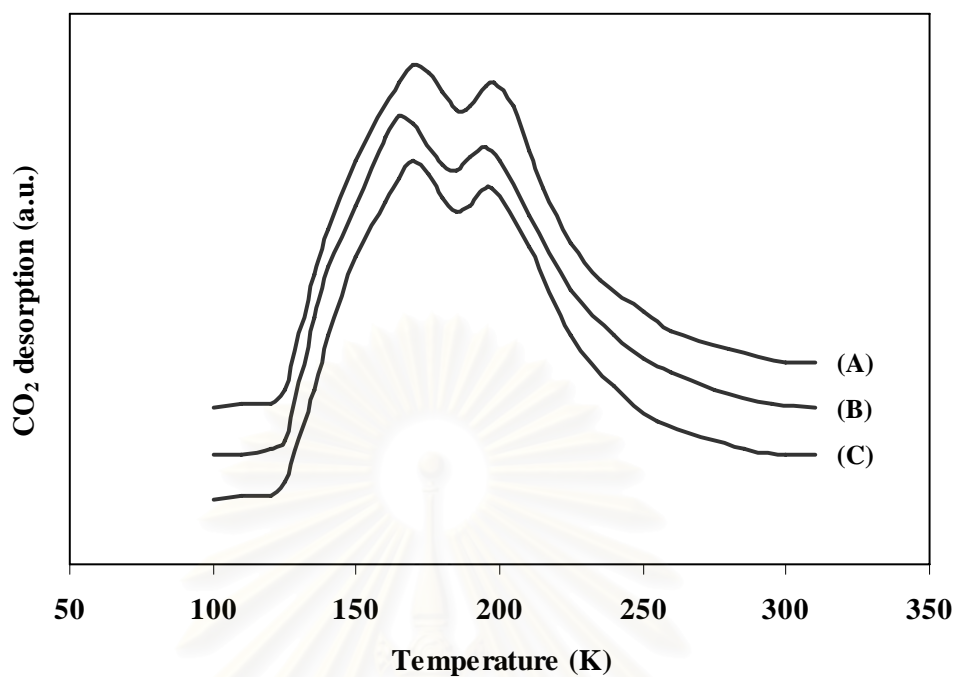


Figure 5.7 Thermal desorption spectra for CO₂ adsorbed on TiO₂ quenched in air at different temperature; (A) Air at 77 K, (B) Air at RT, (C) Air at 373 K

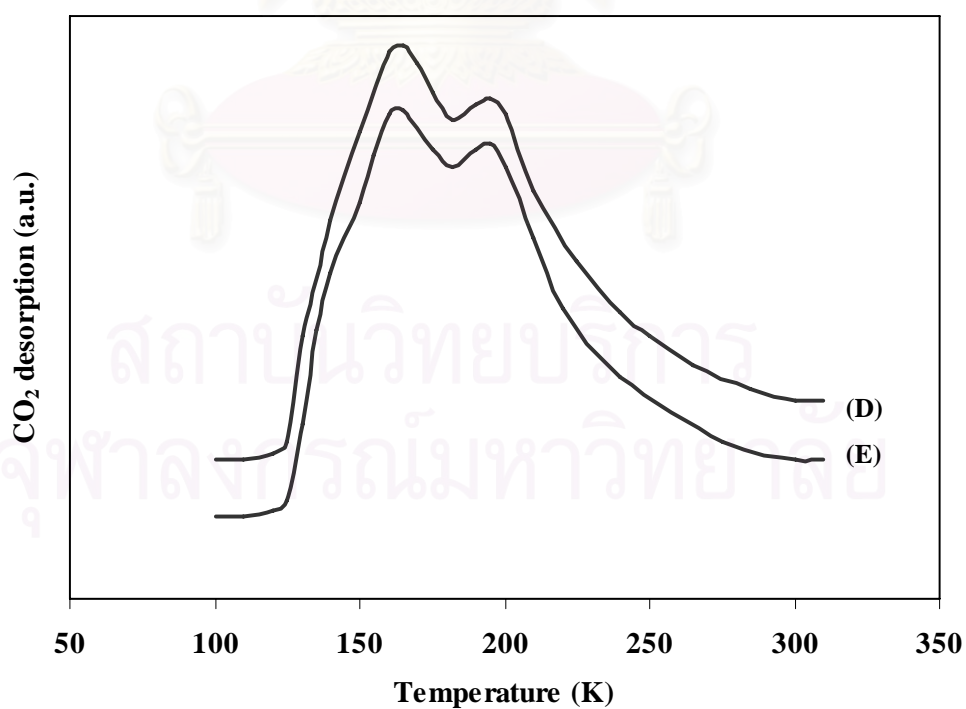


Figure 5.8 Thermal desorption spectra for CO₂ adsorbed on TiO₂ quenched in 30% wt hydrogen peroxide at different temperature; (D) 30% wt H₂O₂ at RT, (E) 30% wt H₂O₂ at 373 K

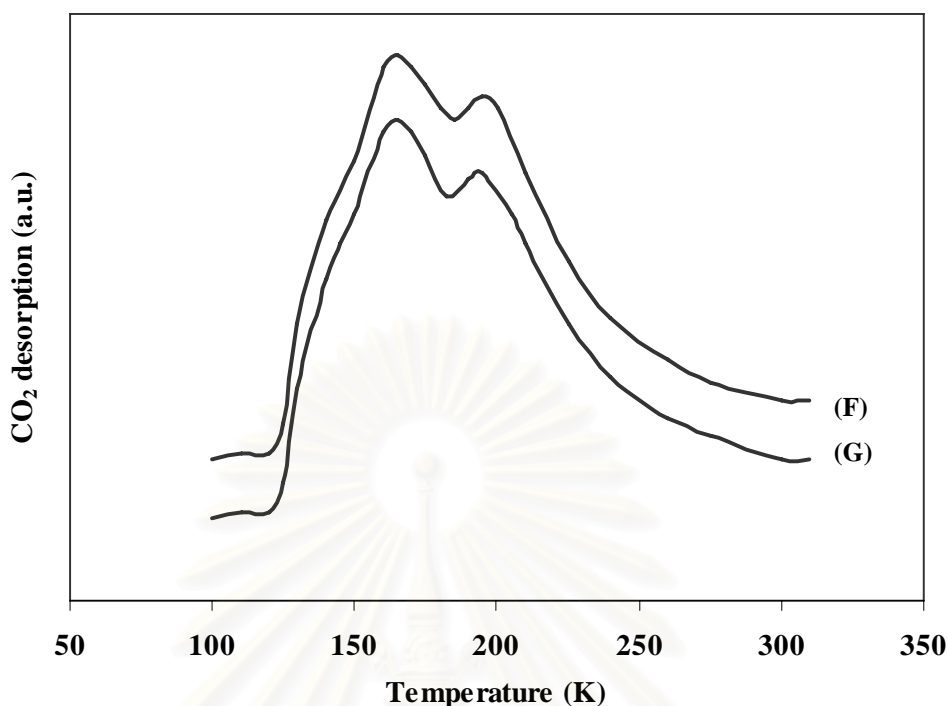


Figure 5.9 Thermal desorption spectra for CO₂ adsorbed on TiO₂ quenched in water at different temperature; (F) H₂O at RT, (G) H₂O at 373 K

The comparing of the amount of Ti³⁺ surface defects of TiO₂ were also determined from the CO₂-TPD and the ESR measurements. Also that shown in the Table 5.4, it was found the amount of Ti³⁺ surface defects of TiO₂ from CO₂-TPD be relative to ESR measurements, it was found that TiO₂ samples quenched in cooler media exhibited higher amount of Ti³⁺ surface defects than those quenched in hotter ones.

The results in Figure 5.10 and 5.11 were shown the amount of Ti³⁺ surface defects and different temperature in various media (i.e., in Air, 30% wt H₂O₂ and H₂O) determined from the CO₂-TPD and the ESR measurements. It was found that TiO₂ samples quenched in cooler media exhibited higher amount of Ti³⁺ surface defects than those quenched in hotter ones. It can be proposed that dependent in terms of the thermal shock effect. The large difference in temperature between media and TiO₂ surface may lead to modification of the surface properties by increasing the amount of Ti³⁺ surface defects on the TiO₂ surface.

Table 5.4 Comparing of the amount of Ti^{3+} surface defects of TiO_2 dependent in terms of the thermal shock effect were also determined from the CO_2 -TPD and the ESR measurements

Samples	Quenching media	Ratio of peak areas of Ti^{3+}/Ti^{4+}	Intensity of Ti^{3+} surface defects per surface area
A	Air at 77 K	0.2479	356.7
B	Air at RT	0.2330	301.9
C	Air at 373 K	0.2225	247.4
D	30% wt H_2O_2 at RT	0.2201	241.9
E	30% wt H_2O_2 at 373 K	0.2173	179.5
F	H_2O at RT	0.2103	141.4
G	H_2O at 373 K	0.2005	128.7

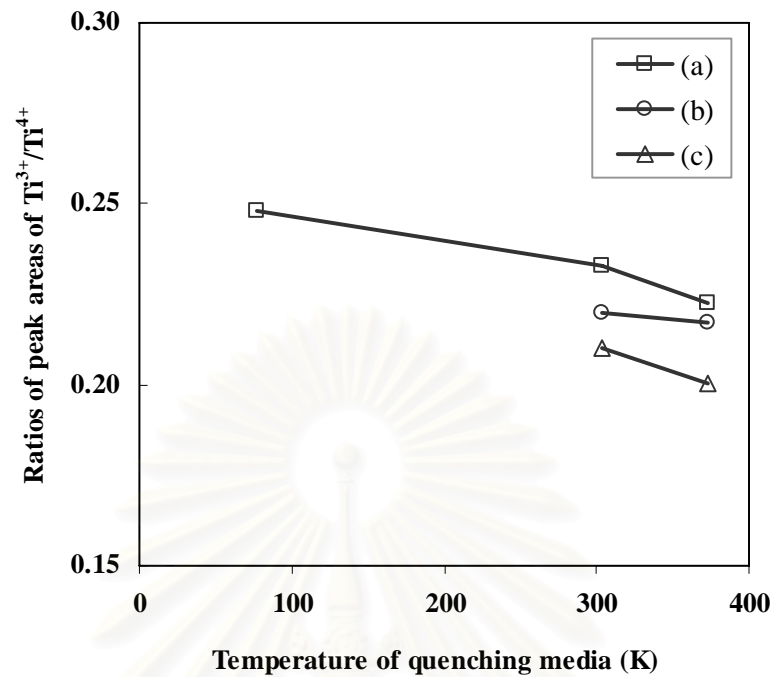


Figure 5.10 Ratios of peak areas of Ti³⁺/Ti⁴⁺ and different temperature in various media; (a) Air, (b) 30% wt H₂O₂ and (c) H₂O

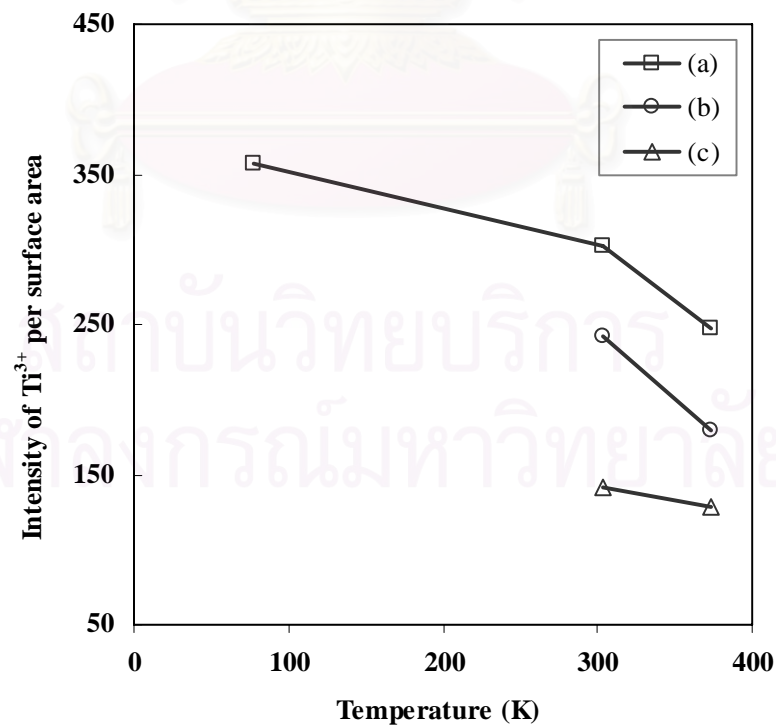


Figure 5.11 Intensity of Ti³⁺ surface defects per surface area and different temperature in various media; (a) Air, (b) 30% wt H₂O₂ and (c) H₂O

5.3.2 Effect of different the quenching media on surface defect

The quenching process had significant directly effect on surface property of TiO_2 . So we can use quenching method for reform surface defect. One of conditions which well knowledge as directly effect to defect structure.

From the CO_2 -TPD results in this study, however, emphasize the influence of quenching media for quenching pre-treatment process of TiO_2 . It is revealed that selected quenching pre-treatment processes can modify the surface properties of TiO_2 . In other words, type of the quenching media has a significant impact on the amount of Ti^{3+} surface defects on the TiO_2 . The results in Figure 5.12 and 5.13 were shown thermal desorption spectra for CO_2 adsorbed on TiO_2 quenched in different the quenching media at room temperature and 373 K, respectively. The results were found to be the TiO_2 quenched in air showed much higher amount of Ti^{3+} surface defects on the TiO_2 than those quenched in hydrogen peroxide and water, respectively. These results can probably be explained in terms of % water in the quenching media, which reported that % water in the quenching media to be in the order: air, 30% wt hydrogen peroxide and water were ca. 4%, 60% and 100% respectively.

The amount of Ti^{3+} surface defect and % water in various quenching media were presented in Figure 5.14 and 5.15. It were shown that amount of Ti^{3+} surface defects on the TiO_2 can be proposed that dependent on terms of % water in the quenching media.

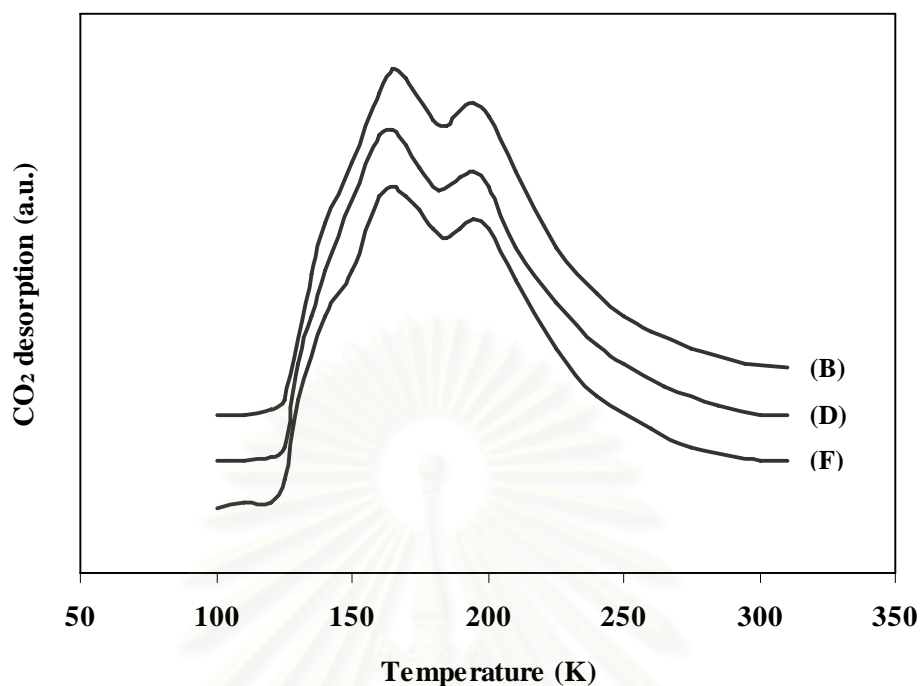


Figure 5.12 Thermal desorption spectra for CO_2 adsorbed on TiO_2 quenched in different the quenching media at room temperature; (B) Air at RT, (D) 30% wt H_2O_2 at RT and (F) H_2O at RT

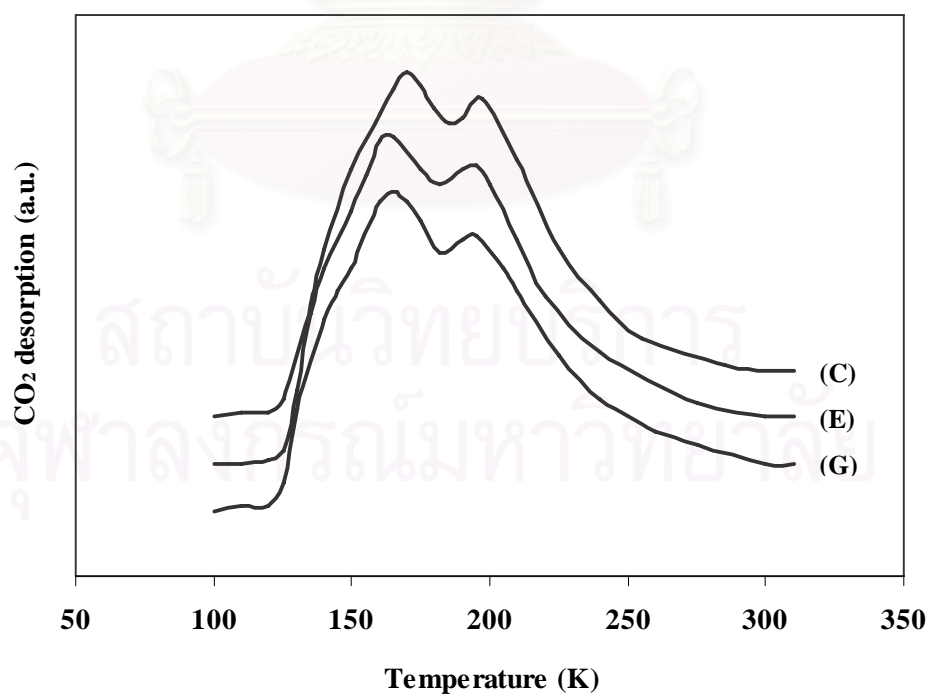


Figure 5.13 Thermal desorption spectra for CO_2 adsorbed on TiO_2 quenched in different the quenching media at 373 K; (C) Air at 373 K, (E) 30%wt H_2O_2 at 373 K and (G) H_2O at 373 K

Table 5.5 Comparing of the amount of Ti^{3+} surface defects of TiO_2 dependent on the % water in quenching media were also determined from the CO_2 -TPD and the ESR measurements

Samples	Quenching media	Ratio of peak areas of Ti^{3+}/Ti^{4+}	Intensity of Ti^{3+} surface defects per surface area
B	Air at RT	0.2330	301.9
D	30% wt H_2O_2 at RT	0.2201	241.9
F	H_2O at RT	0.2103	141.4
C	Air at 373 K	0.2225	247.4
E	30% wt H_2O_2 at 373 K	0.2173	179.5
G	H_2O at 373 K	0.2005	128.7

The comparing of the amount of Ti^{3+} surface defects of TiO_2 were also determined from the CO_2 -TPD and the ESR measurements were also shown in the Table 5.5, it was found the amount of Ti^{3+} surface defects of TiO_2 from CO_2 -TPD be relative to ESR measurements, it was found that amount of Ti^{3+} surface defects on the TiO_2 can be proposed that dependent on terms of % water in the quenching media.

สถาบันวิทยบริการ
จุฬาลงกรณ์มหาวิทยาลัย

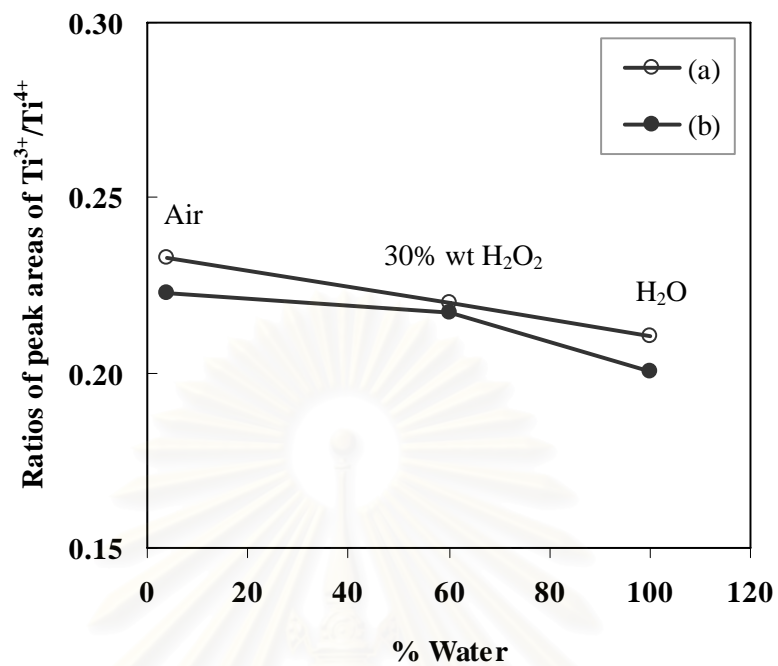


Figure 5.14 Ratios of peak areas of Ti^{3+}/Ti^{4+} and % water in air, 30% wt H_2O_2 and H_2O ; (a) at RT and (b) at 373 K

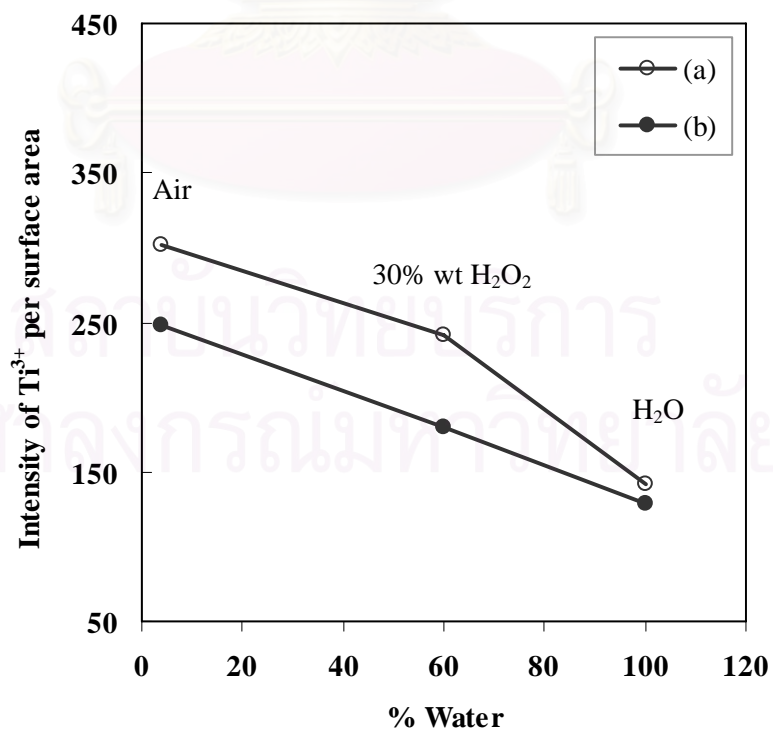


Figure 5.15 Intensity of Ti^{3+} surface defects per surface area and % water in air, 30% wt H_2O_2 and H_2O ; (a) at RT and (b) at 373 K

5.4 Photocatalytic activity of the TiO₂ quenched in various media

The photocatalytic activity of TiO₂ catalysts is still unknown, except for a few important factors such as the magnitude of the band gap, surface area and crystallinity (Park et al. 1999). Because the results in the first part reported that indicating, quenching process of the modification TiO₂ is not influence to crystallite sizes and surface area of TiO₂. Thus, UV-visible absorption measurement was used to perform band gap energy of TiO₂ quenched in the various media. UV-visible spectra of TiO₂ quenched in various media were shown in Table 5.6, it were found that band gap energy is not influence to photocatalytic activity. It can be concluded the amount of Ti³⁺ surface defects on the TiO₂ samples influence to photocatalytic activity, in which the higher amount of Ti³⁺ surface defects present in TiO₂, the higher photocatalytic activity was obtained.

Table 5.6 The band gap energy of TiO₂ quenched in various media

Sample	Quenching media	Band gap energy (eV)
A	Air at 77 K	3.38
B	Air at RT	3.38
C	Air at 373 K	3.37
D	30% wt H ₂ O ₂ at RT	3.37
E	30% wt H ₂ O ₂ at 373 K	3.37
F	H ₂ O at RT	3.36
G	H ₂ O at 373 K	3.36
H (TiO ₂)	-	3.39

Photocatalytic of water decomposition to hydrogen was conducted to assess the photocatalytic activity of the TiO₂ samples quenched in various media and quenching conditions. The performances of hydrogen production of TiO₂ prepared with different quenching media were found to be in the order: Air at 77 K > Air at RT > Air at 373 K > 30% wt H₂O₂ at RT = 30% wt H₂O₂ at 373 K > H₂O at RT > H₂O at 373 K. The results are shown in Figure 5.16 and 5.17 suggest that photocatalytic activity of the nano-sized TiO₂ quenched in different media is evidently different.

In photocatalysis, light irradiation of TiO₂ powder with photon energy larger than the band-gap energy produces electrons (e⁻) and holes (h⁺) in the conduction band and the valence band, respectively. These electrons and holes are thought to have the respective abilities to reduce and oxidize chemical species adsorbed on the surface of TiO₂ particles. For a photocatalyst to be most efficient, different interfacial electron processes involving e⁻ and h⁺ must compete effectively with the major deactivation processes involving e⁻-h⁺ recombination. Many researchers were reported that the modification of TiO₂ surface states can increased the photocatalytic activity and was explained by the increase in Ti³⁺ surface defects of modified TiO₂. Park et al. (Park et al. 1999) reported that the photoelectrons were trapped by the surface defects (Ti³⁺) leading to inhibition of the e⁻-h⁺ recombination. Hence, based on this present study, the roles of surface defects (Ti³⁺) sites on this photocatalytic reaction can be proposed that they acted as trapping photoelectron sites. This suggests, to a certain extent, that the more there are Ti³⁺ on the surface of TiO₂, the better the photocatalytic activity displayed.

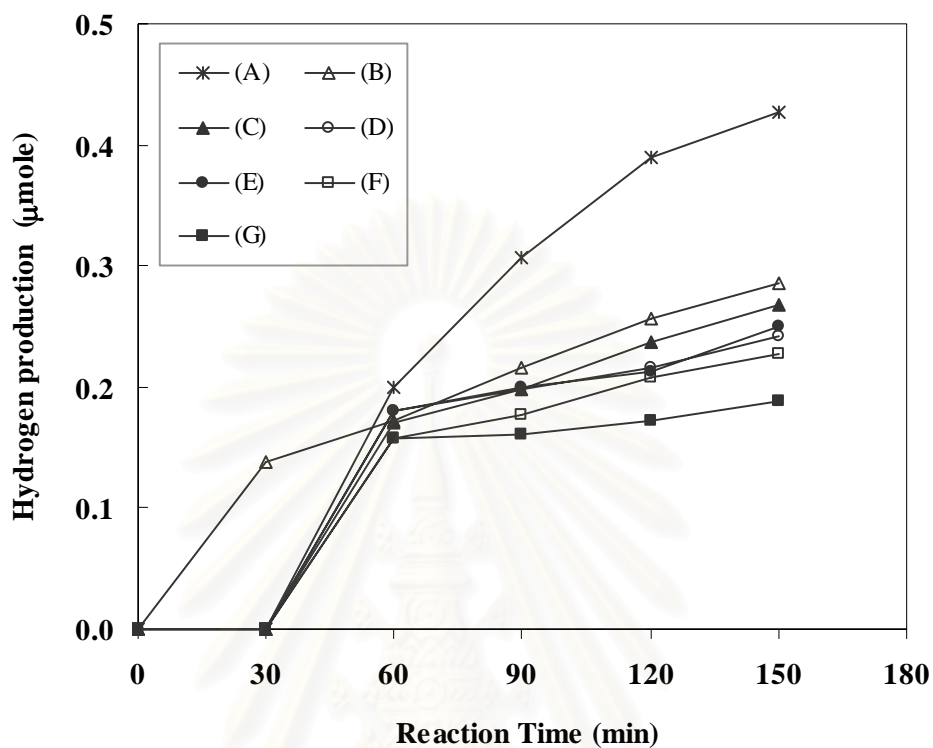


Figure 5.16 Results of photocatalytic testing comparing the activities of TiO₂ quenched in different media; (A) Air at 77 K, (B) Air at RT, (C) Air at 373 K, (D) 30% wt H₂O₂ at RT, (E) 30% wt H₂O₂ at 373 K, (F) H₂O at RT and (G) H₂O at 373 K

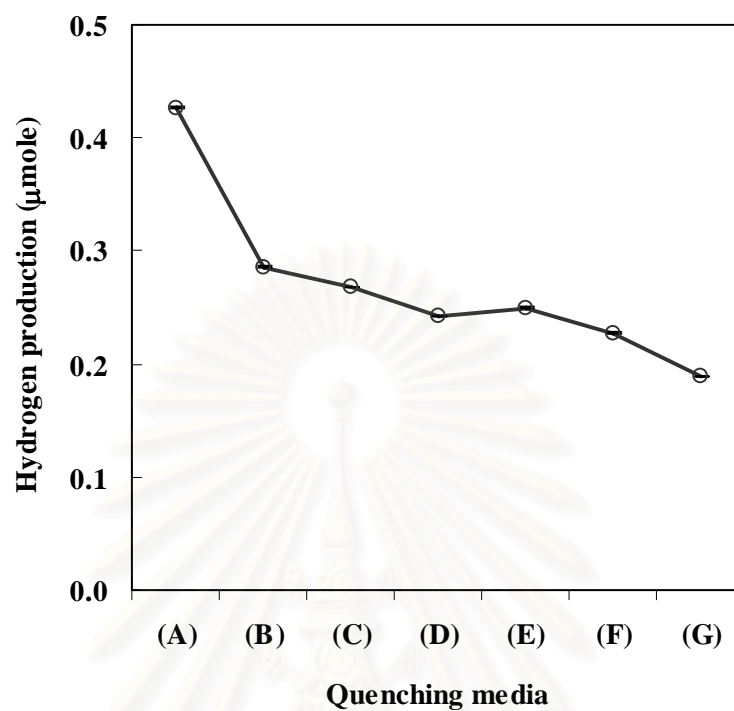


Figure 5.17 Results of photocatalytic testing comparing the activities of TiO_2 quenched in different media; (A) Air at 77 K, (B) Air at RT, (C) Air at 373 K, (D) 30% wt H_2O_2 at RT, (E) 30% wt H_2O_2 at 373 K, (F) H_2O at RT and (G) H_2O at 373 K

5.4.1 Effect of temperature for the quenching media on photocatalytic activity

The results in this study, however, emphasize the influence of quenching condition and media on photocatalytic activity of TiO_2 . It is revealed that selected quenching pre-treatment processes can modify the surface properties of TiO_2 and hence the photocatalytic activity of TiO_2 can be enhanced. In other words, temperature of the quenching media has a significant impact on the amount of Ti^{3+} surface defects on the TiO_2 . Considering the TiO_2 samples quenched in the same type of quenching media (i.e., in Air, 30% wt H_2O_2 and H_2O), it was found that TiO_2 samples quenched in cooler media exhibited higher photocatalytic activity than those quenched in hotter ones.

The results in Figure 5.18 and 5.20 were shown the efficient of hydrogen production from photocatalytic reaction, comparing the activities of TiO_2 quenched in different temperature of the quenching media in air and water respectively, it observed TiO_2 quenched in air at 77 K showed much higher hydrogen production than the one quenched in air at room temperature and air at 373 K, respectively. In other words, TiO_2 quenched in water at room temperature showed much higher hydrogen production than the one quenched at 373 K. These results can probably be explained in terms of the thermal shock effect. The large difference in temperature between media and TiO_2 surface may lead to modification of the surface properties by increasing the amount of Ti^{3+} surface defects on the TiO_2 surface, which as directly effect to increasing the hydrogen production.

Results of photocatalytic testing comparing the activities of TiO_2 quenched in different temperature of the quenching media in hydrogen peroxide were presented in Figure 5.19. It was shown that activity of photocatalytic reaction can be proposed that not dependent in terms of the thermal shock effect.

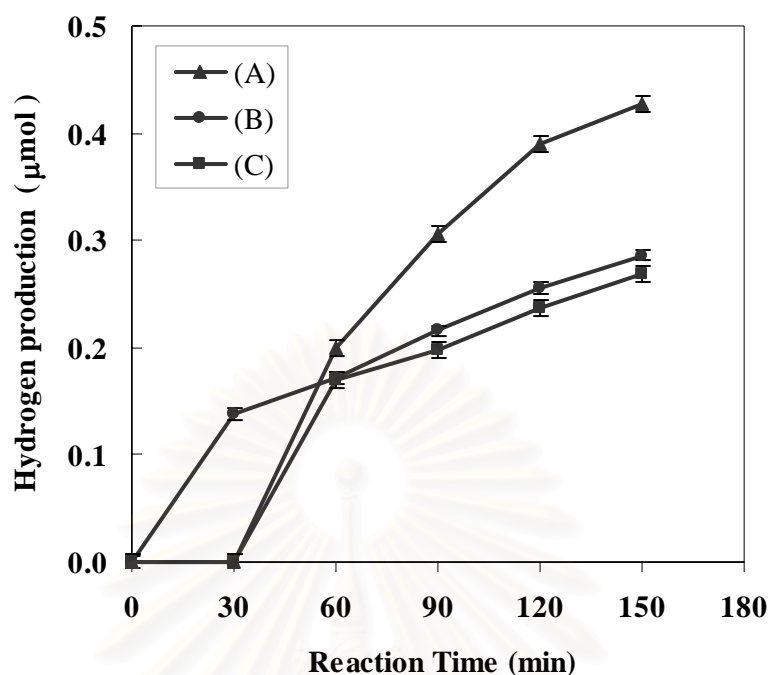


Figure 5.18 Results of photocatalytic testing comparing the activities of TiO₂ quenched in different temperature of the quenching media in air; (A) Air at 77 K, (B) Air at RT and (C) Air at 373 K

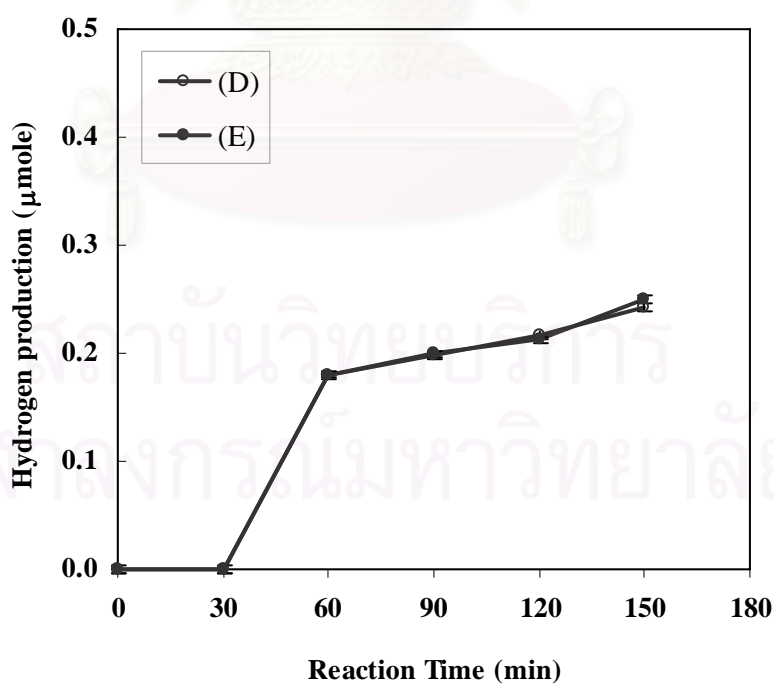


Figure 5.19 Results of photocatalytic testing comparing the activities of TiO₂ quenched in different temperature of the quenching media in hydrogen peroxide; (D) 30% wt H₂O₂ at RT and (E) 30% wt H₂O₂ at 373 K

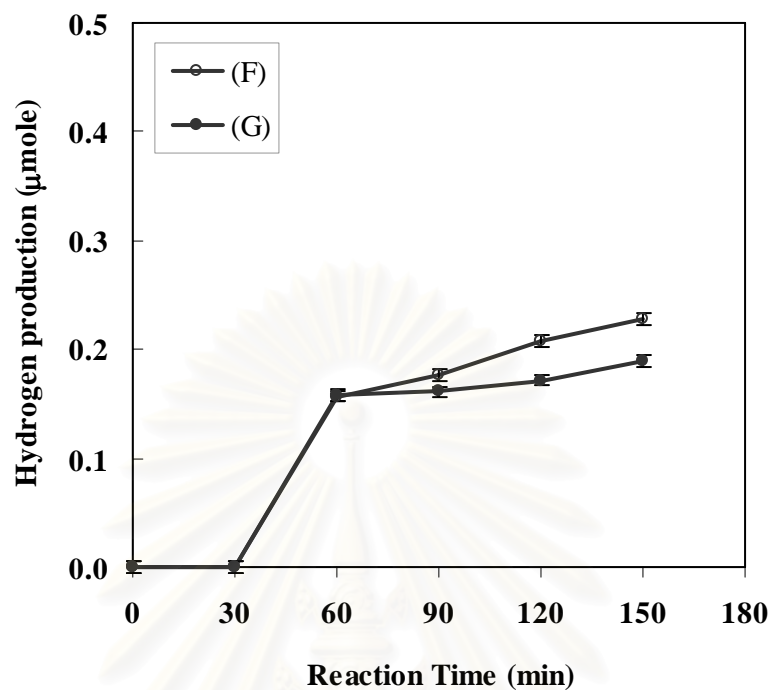


Figure 5.20 Results of photocatalytic testing comparing the activities of TiO₂ quenched in different temperature of the quenching media in water; (F) H₂O at RT and (G) H₂O at 373 K

5.4.2 Effect of different the quenching media on photocatalytic activity

The quenching process had significant directly effect on surface property of TiO_2 . So we can use quenching method for reform surface defect, which hydrogen production from photocatalytic reaction had better. One of conditions which well knowledge as directly effect to photocatalytic activity is defect structure.

The results in Figure 5.21 and 5.22 were shown the efficient of hydrogen production from photocatalytic reaction, comparing the activities of TiO_2 quenched in different the quenching media at room temperature and 373 K, respectively. The results were found to be the TiO_2 quenched in air showed much higher hydrogen production than those quenched in hydrogen peroxide and water, respectively. These results can probably be explained in terms of % water in the quenching media, which reported that % water in the quenching media to be in the order: air, 30% wt hydrogen peroxide and water were ca. 4%, 60% and 100% respectively.

Results of photocatalytic testing comparing the activities of TiO_2 quenched in various media and % water were presented in Figure 5.23. It was shown that activity of photocatalytic reaction can be proposed that dependent on terms of % water in the quenching media.

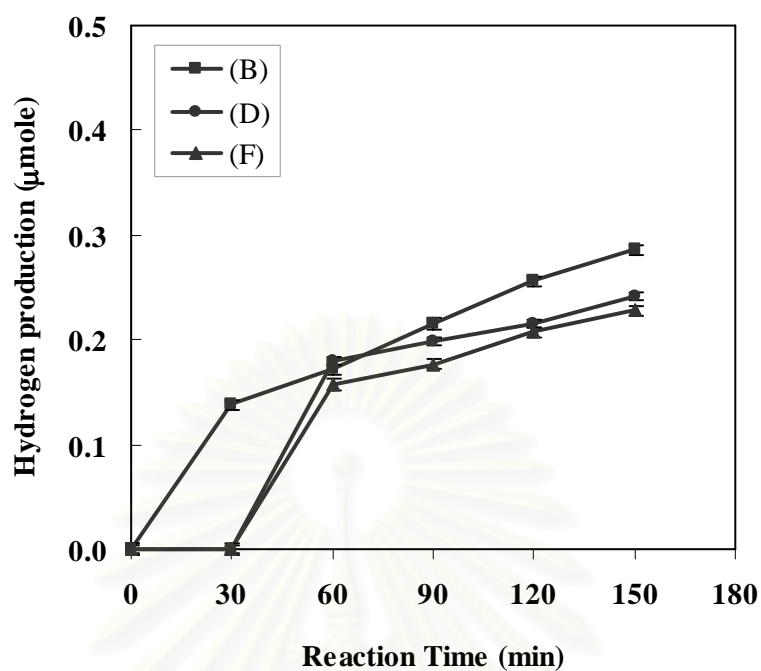


Figure 5.21 Results of photocatalytic testing comparing the activities of TiO₂ quenched in different the quenching media at room temperature; (B) Air at RT, (D) 30% wt H₂O₂ at RT and (F) H₂O at RT

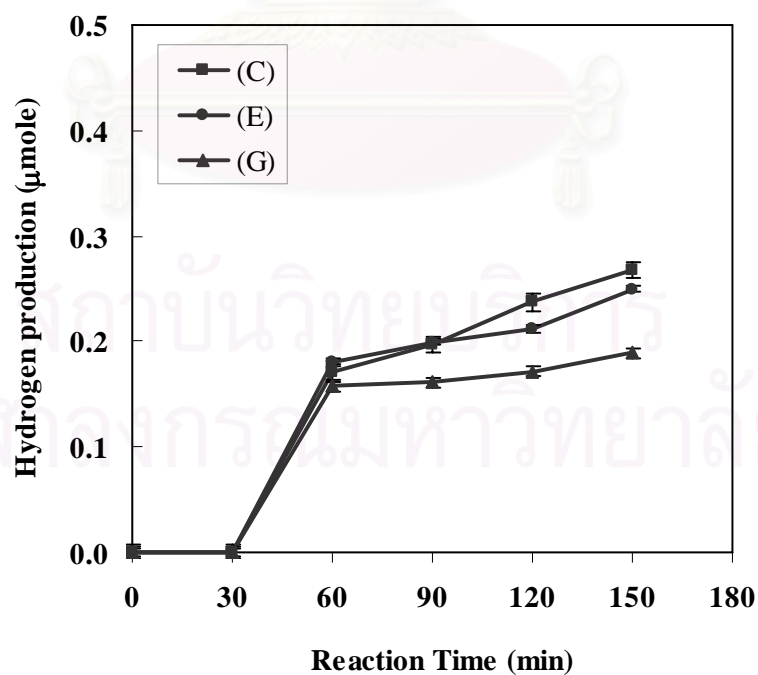


Figure 5.22 Results of photocatalytic testing comparing the activities of TiO₂ quenched in different the quenching media at 373 K; (C) Air at 373 K, (E) 30%wt H₂O₂ at 373 K and (G) H₂O at 373 K

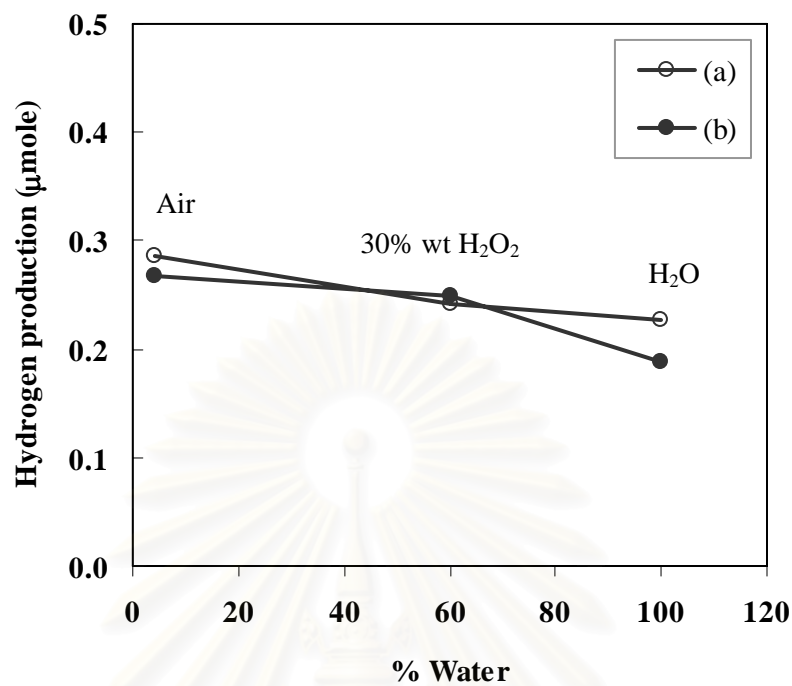


Figure 5.23 Results of photocatalytic testing comparing the activities of TiO₂ quenched in various media and % water of air, 30% wt H₂O₂ and H₂O; (a) at RT and (b) at 373 K

..

สถาบันวิทยบริการ
จุฬาลงกรณ์มหาวิทยาลัย

5.5 Photocatalytic Reaction

From the results of photocatalytic reaction on TiO₂ quenched in the various media were found to be that difference to start of the reaction. The results are shown in Figure 5.24 exhibited two times to start of the reaction, it was observed that earlier and later to start of the reaction.

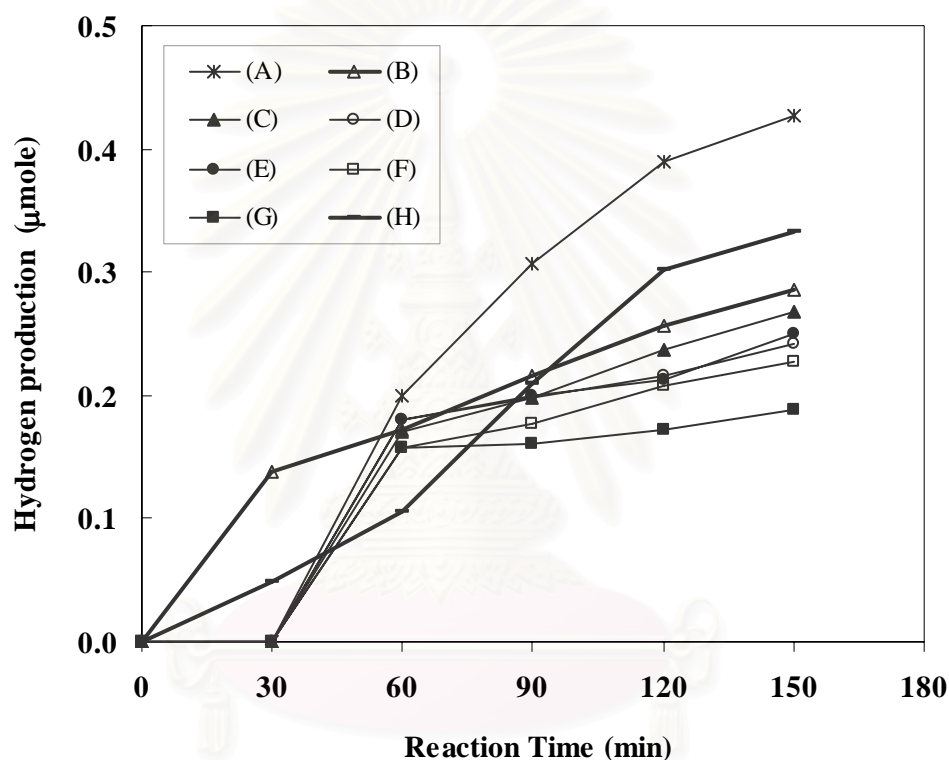


Figure 5.24 Results of photocatalytic testing comparing the activities of TiO₂ quenched in different media; (A) Air at 77 K, (B) Air at RT, (C) Air at 373 K, (D) 30% wt H₂O₂ at RT, (E) 30% wt H₂O₂ at 373 K, (F) H₂O at RT, (G) H₂O at 373 K and (H) TiO₂

Thus, UV-visible absorption measurement, Thermal gravimetric analysis and Fourier-Transform Infrared spectroscopy were used for performed to determine the band gap energy, the organic compound on the surface and functional group on the surface respectively, of TiO₂ quenched in the various media.

5.5.1 UV-visible absorption measurement

UV-visible absorption analysis is the most common procedure for determining diffuse reflectance spectra the TiO_2 . Because of the photocatalytic activity dependent on band gap energy and photocatalytic reaction results, there were observed that earlier and later to start of the reaction. Thus, UV-visible absorption measurement was used to perform band gap energy of TiO_2 quenched in the various media. UV-visible spectra of TiO_2 quenched in various media were shown in Figure 5.25, we examine the diffuse reflectance spectra of TiO_2 in the range of 280-500 nm. The band gap energy of TiO_2 quenched in various media in the Table 5.7, which determined by Tauc plot.

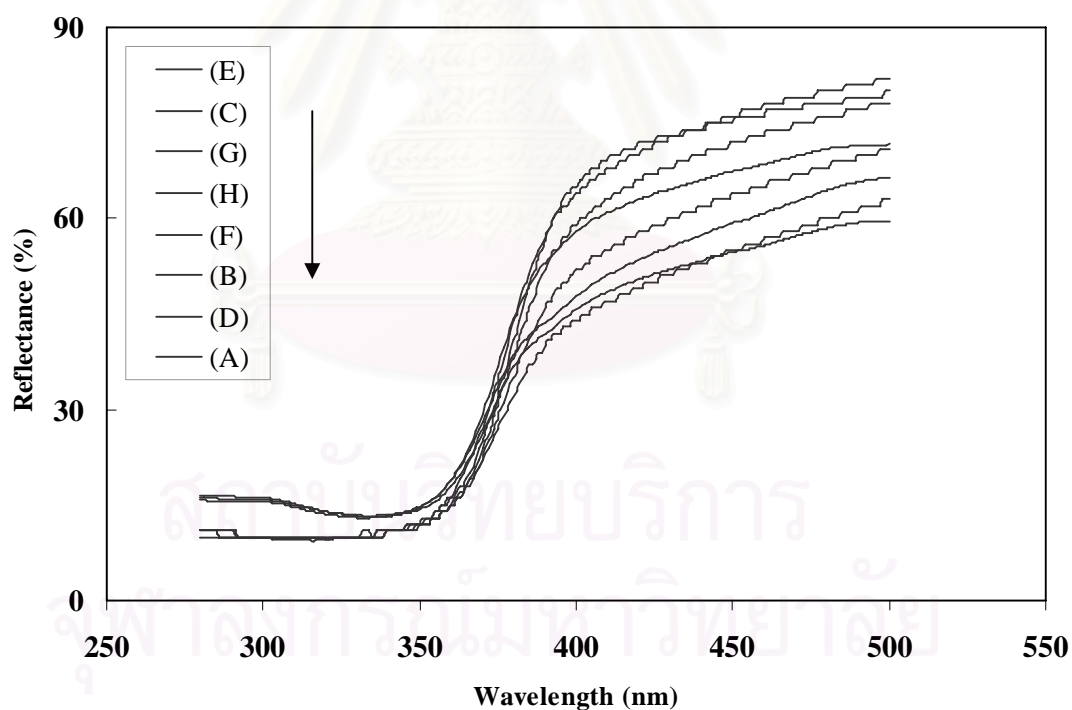


Figure 5.25 The UV- vis spectra of TiO_2 quenched in different media; (A) Air at 77 K, (B) Air at RT, (C) Air at 373 K, (D) 30% wt H_2O_2 at RT, (E) 30% wt H_2O_2 at 373 K, (F) H_2O at RT, (G) H_2O at 373 K and (H) TiO_2

Table 5.7 The band gap energy of TiO₂ quenched in various media

Sample	Quenching media	Band gap energy (eV)
A	Air at 77 K	3.38
B	Air at RT	3.38
C	Air at 373 K	3.37
D	30% wt H ₂ O ₂ at RT	3.37
E	30% wt H ₂ O ₂ at 373 K	3.37
F	H ₂ O at RT	3.36
G	H ₂ O at 373 K	3.36
H (TiO ₂)	-	3.39

The results reported in the Table 5.7 suggest that to have band gap energy of TiO₂ samples quenched in various media to be equivalent. Therefore, can also be ascribed to the start of the photocatalytic reaction on TiO₂ quenched in various media was not because of band gap energy of TiO₂.

สถาบันวิทยบริการ
จุฬาลงกรณ์มหาวิทยาลัย

5.5.2 Thermal gravimetric Analysis (TGA)

Thermal gravimetric analysis is the most common procedure for determining the organic compound on the surface of catalyst. TGA experiment was used to perform organic compound on the surface of TiO_2 quenched in the various media. Because of the photocatalytic reaction results, there were observed that earlier and later to start of the reaction. The TGA profiles of TiO_2 quenched in the various media under oxygen flow 100 ml/min, a heating rate of $10\text{ }^\circ\text{C}/\text{min}$ from temperature of 25 to $700\text{ }^\circ\text{C}$ was reported in Figure 5.26. The results reported suggest that to have organic compound on the TiO_2 surface samples quenched in various media to be equivalent. Therefore, can also be ascribed to the start of the photocatalytic reaction on TiO_2 quenched in various media were not because of organic compound on the TiO_2 surface.

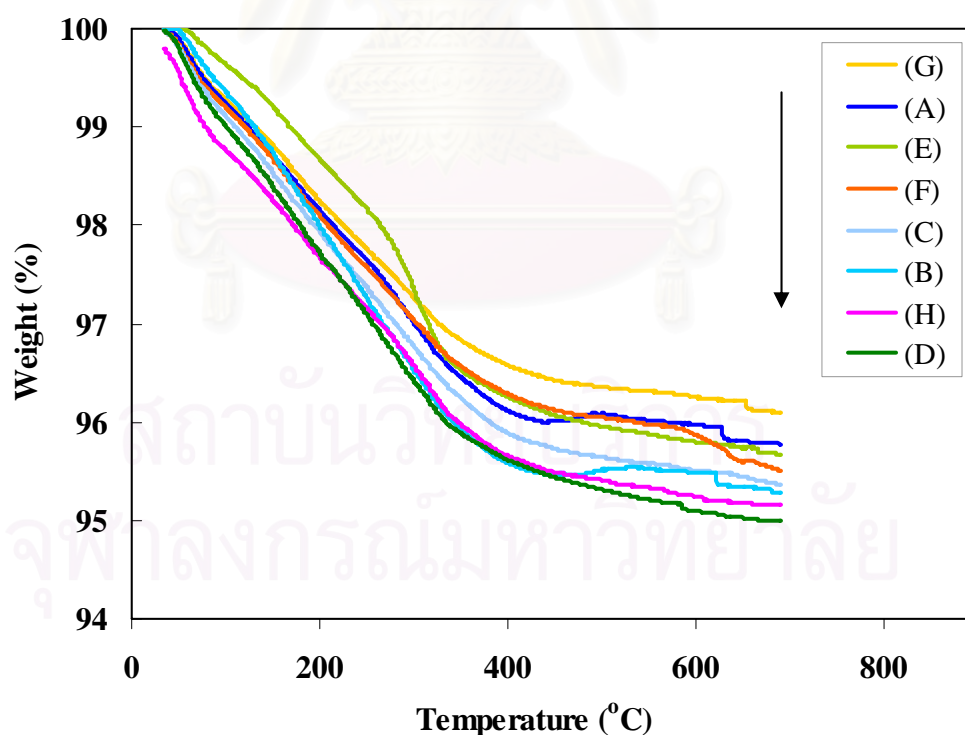


Figure 5.26 The TGA profiles of TiO_2 quenched in different media; (A) Air at 77 K, (B) Air at RT, (C) Air at 373 K, (D) 30% wt H_2O_2 at RT, (E) 30% wt H_2O_2 at 373 K, (F) H_2O at RT, (G) H_2O at 373 K and (H) TiO_2

5.5.3 Fourier-Transform Infrared Spectroscopy (FT-IR)

The results in Figure 5.27, it can be identification of the surface hydroxyl modes by IR spectroscopy is problematic because they appear in the range of 3730-3750 cm^{-1} . It found to the region of the spectral position of $\sim 3664 \text{ cm}^{-1}$ to deformation vibrations of hydroxyl groups on the TiO_2 surface, quenched in the various media for the photocatalytic reaction observed that later to start of the reaction, because of the bridging hydroxyl group and water on the TiO_2 surface leading to inhabitation effective site (Ti^{3+} sites) for photocatalytic reaction. However, the start of the reaction of TiO_2 quenched in the hydrogen peroxide at 373 K observed that later to start of the reaction caused by relation has the region of the spectral position of $\sim 3560 \text{ cm}^{-1}$, it can be described in the same cause.

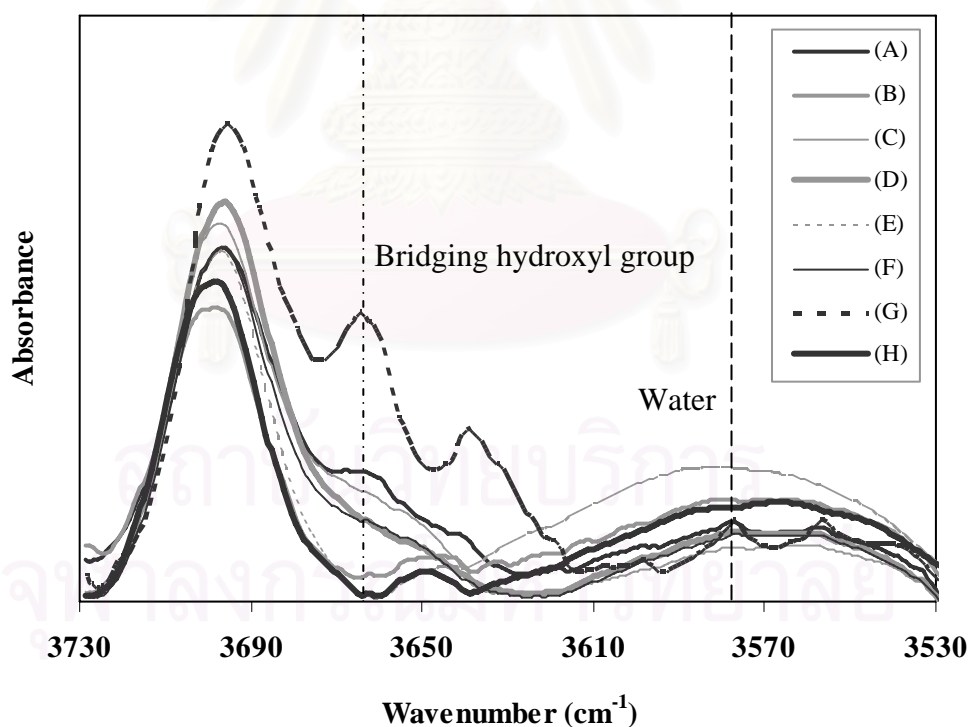


Figure 5.27 The IR spectra of TiO_2 quenched in different media; (A) Air at 77 K, (B) Air at RT, (C) Air at 373 K, (D) 30% wt H_2O_2 at RT, (E) 30%wt H_2O_2 at 373 K, (F) H_2O at RT, (G) H_2O at 373 K and (H) TiO_2

The photocatalytic reaction results, there were observed that earlier and later to start of the reaction. Therefore, can also be ascribed to the start of the photocatalytic reaction on TiO_2 quenched in various media were not because of band gap energy of TiO_2 and organic compound on the TiO_2 surface, but because of bridging hydroxyl group and water on the TiO_2 surface leading to inhabitation effective site (Ti^{3+} sites) for photocatalytic reaction.



สถาบันวิทยบริการ
จุฬาลงกรณ์มหาวิทยาลัย

CHAPTER VI

CONCLUSIONS AND RECOMMENDATIONS

6.1 Conclusions

In this work, to study the surface properties and photocatalytic activities of nano-sized TiO_2 powders synthesized by solvothermal method can be significantly influenced by quenching media and quenching conditions. The conclusions of the present research are the following:

1. For quenching immediately after calcined was increasing amount of Ti^{3+} on surface of catalyst and exhibited increasing photocatalytic activity.
2. For quenching in a similar medium, TiO_2 quenched in cooler media exhibited higher photocatalytic activity than those quenched in hotter ones.
3. For room temperature quenching, the photocatalytic activities of TiO_2 quenched in air exhibited higher activity than those quenched in 30 wt% H_2O_2 and H_2O , respectively.
4. The start of the photocatalytic reaction on TiO_2 quenched in various media because of bridging hydroxyl group and water on the TiO_2 surface leading to inhabitation effective site (Ti^{3+} sites) for photocatalytic reaction.

6.2 Recommendations

Quenching process has been shown in this work to be a useful technique for surface modification of nano-sized TiO_2 powders in order to enhance their photocatalytic activity. Some recommendations for future work are listed as follows:

1. From result of IR spectroscopy can be identify to peak at the spectral position of $\sim 3650 \text{ cm}^{-1}$ by other characterization which should be further investigated.

2. For the photocatalytic reaction, photocatalytic activity for water decomposition to hydrogen. Improvement the operating conditions for each instrument and additional parameters including reaction time and condition of reaction should be investigated.



สถาบันวิทยบริการ
จุฬาลงกรณ์มหาวิทยาลัย

REFERENCES

- Amama, P. B., Itoh, K., and Murabayashi, M. (2002). "Gas-phase photocatalytic degradation of trichloroethylene on pretreated TiO₂." *Applied Catalysis B-Environmental*, 37(4), 321.
- Boyer, H. E. (1988). "Quenching and Control of Distortion." *ASM International, Ohio*.
- Calatayud, M., Markovits, A., and Minot, C. (2004). "Electron-count control on adsorption upon reducible and irreducible clean metal-oxide surfaces." *Catalysis Today*, 89(3), 269-278.
- Chen, J., Ollis, D. F., Rulkens, W. H., and Bruning, H. (1999). "Photocatalyzed oxidation of alcohols and organochlorides in the presence of native TiO₂ and metallized TiO₂ suspensions. Part (II): Photocatalytic mechanisms." *Water Research*, 33(3), 669-676.
- Deng, X. Y., Yue, Y. H., and Gao, Z. (2002). "Gas-phase photo-oxidation of organic compounds over nanosized TiO₂ photocatalysts by various preparations." *Applied Catalysis B-Environmental*, 39(2), 135.
- Diebold, U. (2003). "The surface science of titanium dioxide." *Surface Science Reports*, 48(5-8), 53.
- Henderson, M. A. (1996). "An HREELS and TPD study of water on TiO₂(110): The extent of molecular versus dissociative adsorption." *Surface Science*, 355(1-3), 151.
- Herrmann, J. M., Guillard, C., Disdier, J., Lehaut, C., Malato, S., and Blanco, J. (2002). "New industrial titania photocatalysts for the solar detoxification of water containing various pollutants." *Applied Catalysis B-Environmental*, 35(4), 281.
- Horikoshi, S., Hidaka, H., and Serpone, N. (2003). "Hydroxyl radicals in microwave photocatalysis. Enhanced formation of OH radicals probed by ESR techniques in microwave-assisted photocatalysis in aqueous TiO₂ dispersions." *Chemical Physics Letters*, 376(3-4), 475-480.
- Kim, C. S., Moon, B. K., Park, J. H., Chung, S. T., and Son, S. M. (2003a). "Synthesis of nanocrystalline TiO₂ in toluene by a solvothermal route." *Journal of Crystal Growth*, 254(3-4), 405.

- Kim, K. W., Lee, E. H., Kim, Y. J., Lee, M. H., Kim, K. H., and Shin, D. W. (2003b). "A relation between the non-stoichiometry and hydroxyl radical generated at photocatalytic TiO₂ on 4CP decomposition." *Journal of Photochemistry and Photobiology a-Chemistry*, 159(3), 301-310.
- Kongsuebchart, W., Prasertdam, P., Panpranot, J., Sirisuk, A., Supphasrironrojaroen, P., and Satayaprasert, C. (2006). "Effect of crystallite size on the surface defect of nano-TiO₂ prepared via solvothermal synthesis." *Journal of Crystal Growth*, 297(1), 234-238.
- Linsebigler, A. L., Lu, G. Q., and Yates, J. T. (1995). "Photocatalysis on TiO₂ Surfaces - Principles, Mechanisms, and Selected Results." *Chemical Reviews*, 95(3), 735.
- Liu, G., Rodriguez, J. A., Chang, Z., Hrbek, J., and Gonzalez, L. (2002). "Adsorption of methanethiol on stoichiometric and defective TiO₂(110) surfaces: A combined experimental and theoretical study." *Journal of Physical Chemistry B*, 106(38), 9883.
- Liu, H., Ma, H. T., Li, X. Z., Li, W. Z., Wu, M., and Bao, X. H. (2003). "The enhancement of TiO₂ photocatalytic activity by hydrogen thermal treatment." *Chemosphere*, 50(1), 39-46.
- Machado, N., and Santana, V. S. (2005). "Influence of thermal treatment on the structure and photocatalytic activity of TiO₂ P25." *Catalysis Today*, 107-08, 595-601.
- Meng Ni, M. K. H. L., Dennis Y.C. Leung, K. Sumathy. (2005). "A review and recent developments in photocatalytic water-splitting using TiO₂ for hydrogen production." *Renewable and Sustainable Energy Reviews*.
- Moon, S. C., Mametsuka, H., Tabata, S., and Suzuki, E. (2000). "Photocatalytic production of hydrogen from water using TiO₂ and B/TiO₂." *Catalysis Today*, 58(2-3), 126.
- Nakaoka, Y., and Nosaka, Y. (1997). "ESR Investigation into the effects of heat treatment and crystal structure on radicals produced over irradiated TiO₂ powder." *Journal of Photochemistry and Photobiology a-Chemistry*, 110(3), 299.
- Park, D. R., Zhang, J. L., Ikeue, K., Yamashita, H., and Anpo, M. (1999). "Photocatalytic oxidation of ethylene to CO₂ and H₂O on ultrafine powdered TiO₂ photocatalysts in the presence of O⁻² and H₂O." *Journal of Catalysis*, 185(1), 114-119.

- Payakgul, W., Mekasuwandumrong, O., Pavarajarn, V., and Prasertthdam, P. (2005). "Effects of reaction medium on the synthesis of TiO₂ nanocrystals by thermal decomposition of titanium (IV) n-butoxide." *Ceramics International*, 31(3), 391-397.
- Ramirez, J., Cedeno, L., and Busca, G. (1999). "The role of titania support in MO_x based hydrodesulfurization catalysts." *Journal of Catalysis*, 184(1), 59.
- Rusu, C. N., and Yates, J. T. (1997). "Defect sites on TiO₂(110). Detection by O⁻² photodesorption." *Langmuir*, 13(16), 4311.
- Sakata, T., Kawai, T., and Hashimoto, K. (1982). "Photochemical diode model of Pt/TiO₂ particle and its photocatalytic activity" *Chemical Physics Letters*, 88(1), 50-54.
- Shklover, V., Nazeeruddin, M. K., Zakeeruddin, S. M., Barbe, C., Kay, A., Haibach, T., Steurer, W., Hermann, R., Nissen, H. U., and Gratzel, M. (1997). "Structure of nanocrystalline TiO₂ powders and precursor to their highly efficient photosensitizer." *Chemistry of Materials*, 9(2), 430.
- Shultz, A. N., Jang, W., Hetherington, W. M., Baer, D. R., Wang, L. Q., and Engelhard, M. H. (1995). "Comparative 2nd-Harmonic Generation and X-Ray Photoelectron-Spectroscopy Studies of the Uv Creation and O⁻² Healing of Ti³⁺ Defects on (110)Rutile TiO₂ Surfaces." *Surface Science*, 339(1-2), 114-124.
- Suriye, K., Prasertthdam, P., and Jongsomjit, B. (2007). "Control of Ti³⁺ surface defect on TiO₂ nanocrystal using various calcination atmospheres as the first step for surface defect creation and its application in photocatalysis." *Applied Surface Science*, 253, 3849–3855.
- Theinkeaw, S. (2000). "Synthesis of Large-Surface Area Silica Modified Titanium (IV) Oxide Ultra Fine Particles." *Master' s thesis, Department of Chemical Engineering, Graduated School, Chulalongkorn University.*
- Thompson, T. L., Diwald, O., and Yates, J. T. (2003). "CO₂ as a probe for monitoring the surface defects on TiO₂(110) - Temperature-programmed Desorption." *Journal of Physical Chemistry B*, 107(42), 11700.
- Tilocca, A., and Selloni, A. (2004). "Structure and reactivity of water layers on defect-free and defective anatase TiO₂(101) surfaces." *Journal of Physical Chemistry B*, 108(15), 4743.
- Torimoto, T., Fox, R. J., and Fox, M. A. (1996). "Photoelectrochemical doping of TiO₂ particles and the effect of charge carrier density on the photocatalytic activity of microporous semiconductor electrode films." *Journal of the Electrochemical Society*, 143(11), 3712.

- Wang, C. C., and Ying, J. Y. (1999). "Sol-gel synthesis and hydrothermal processing of anatase and rutile titania nanocrystals." *Chemistry of Materials*, 11(11), 3113-3120.
- Wu, N. L., Lee, M. S., Pon, Z. J., and Hsu, J. Z. (2004). "Effect of calcination atmosphere on TiO₂ photocatalysis in hydrogen production from methanol/water solution." *Journal of Photochemistry and Photobiology a-Chemistry*, 163(1-2), 277-280.
- Yin, S., Fujishiro, Y., Wu, J. H., Aki, M., and Sato, T. (2003). "Synthesis and photocatalytic properties of fibrous titania by solvothermal reactions." *Journal of Materials Processing Technology*, 137(1-3), 45.
- Zhang, H. Z., and Banfield, J. F. (2000). "Understanding polymorphic phase transformation behavior during growth of nanocrystalline aggregates: Insights from TiO₂." *Journal of Physical Chemistry B*, 104(15), 3481.



สถาบันวิทยบริการ
จุฬาลงกรณ์มหาวิทยาลัย



APPENDICES

สถาบันวิทยบริการ
จุฬาลงกรณ์มหาวิทยาลัย

APPENDIX A

CALCULATION OF THE CRYSTALLITE SIZE

Calculation of the crystallite size by Debye-Scherrer equation

The crystallite size was calculated from the half-height width of the diffraction peak of XRD pattern using the Debye-Scherrer equation.

From Scherrer equation:

$$D = \frac{K\lambda}{\beta \cos \theta} \quad (\text{A.1})$$

- where
- D = Crystallite size, Å
 - K = Crystallite-shape factor = 0.9
 - λ = X-ray wavelength, 1.5418 Å for CuK α
 - θ = Observed peak angle, degree
 - β = X-ray diffraction broadening, radian

The X-ray diffraction broadening (β) is the pure width of a powder diffraction free of all broadening due to the experimental equipment. Standard α -alumina is used to observe the instrumental broadening since its crystallite size is larger than 2000 Å. The X-ray diffraction broadening (β) can be obtained by using Warren's formula.

From Warren's formula:

$$\beta^2 = B_M^2 - B_S^2 \quad (\text{A.2})$$
$$\beta = \sqrt{B_M^2 - B_S^2}$$

- Where
- B_M = The measured peak width in radians at half peak height.
 - B_S = The corresponding width of a standard material.

Example: Calculation of the crystallite size of titanium dioxide

$$\begin{aligned} \text{The half-height width of 101 diffraction peak} &= 0.93125^\circ \\ &= 0.01625 \text{ radian} \end{aligned}$$

$$\text{The corresponding half-height width of peak of } \alpha\text{-alumina} = 0.002 \text{ radian}$$

$$\begin{aligned} \text{The pure width} &= \sqrt{B_M^2 - B_S^2} \\ &= \sqrt{0.01625^2 - 0.004^2} \\ &= 0.01612 \text{ radian} \end{aligned}$$

$$B = 0.01612 \text{ radian}$$

$$2\theta = 25.46^\circ$$

$$\theta = 12.73^\circ$$

$$\lambda = 1.5418 \text{ \AA}$$

$$\begin{aligned} \text{The crystallite size} &= \frac{0.9 \times 1.5418}{0.0157 \cos 12.73} = 100.5 \text{ \AA} \\ &= 10.05 \text{ nm} \end{aligned}$$

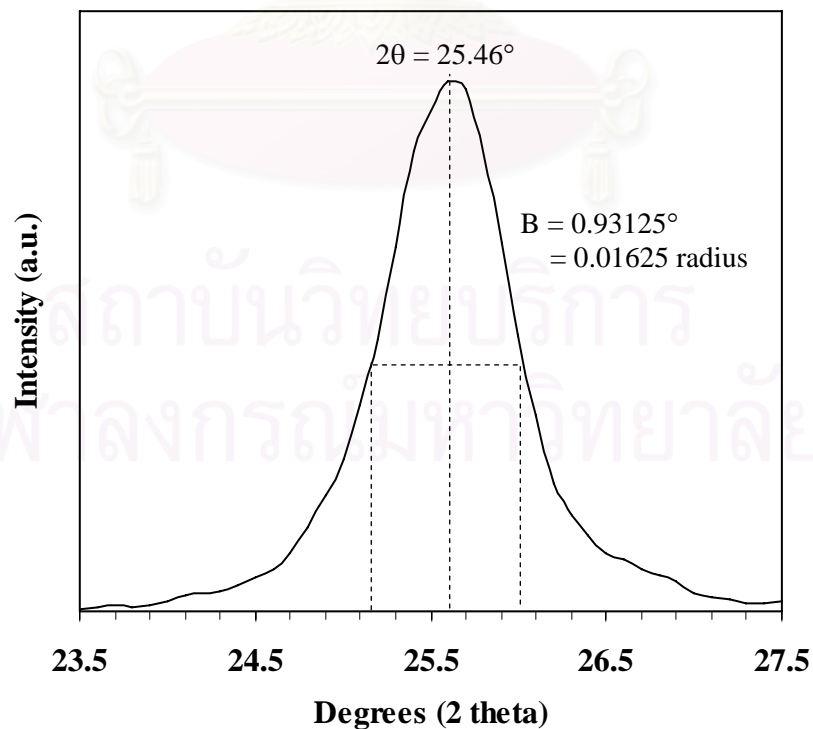


Figure A.1 The 101 diffraction peak of titanium dioxide for calculation of the crystallite size

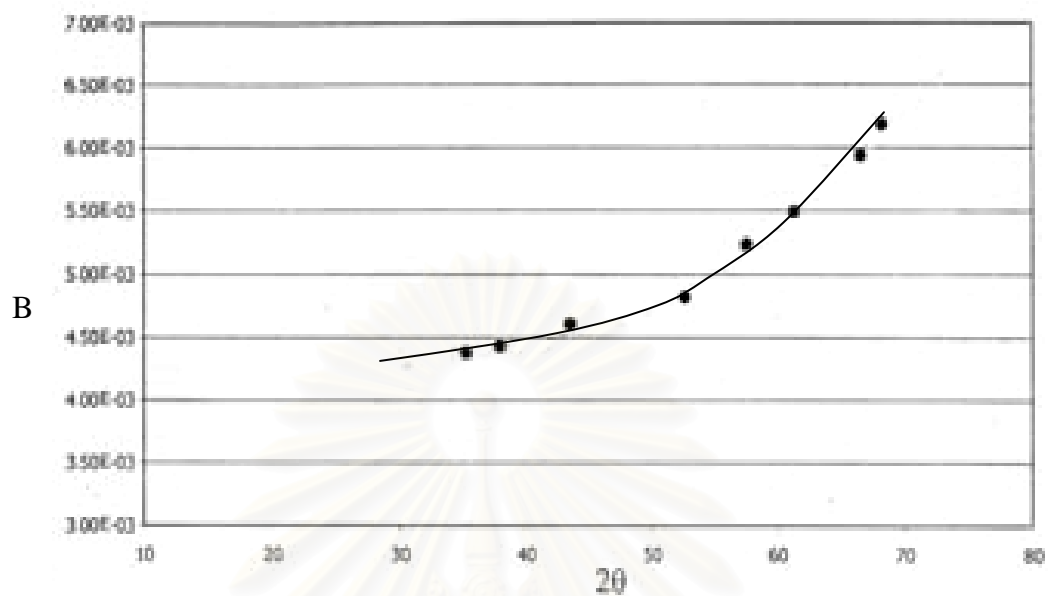


Figure A.2 The plot indicating the value of line broadening due to the equipment. The data were obtained by using α -alumina as standard

สถาบันวิทยบริการ
จุฬาลงกรณ์มหาวิทยาลัย

APPENDIX B

CALIBRATION CURVES

This appendix showed the calibration curves for calculation of products in photocatalytic reaction of water decomposition to hydrogen.

The thermal conductivity detector, gas chromatography Shimadzu model 8A was used to analyze the concentration of hydrogen by using Molecular sieve 5A column. The operating conditions for each instrument are show in the Table B.1

Table B.1 The operating conditions for gas chromatograph

Gas Chromagraph	SHIMADZU GC-8A
Detector	TCD
Column	Molecular sieve 5A
- Column material	SUS
- Length	2 m
- Outer diameter	4 mm
- Inner diameter	3 mm
- Mesh range	60/80
- Maximum temperature	350 °C
Carrier gas	Ar (99.999%)
Carrier gas flow (ml/min)	30 cc/min
Column temperature	
- initial (°C)	60
- final (°C)	60
Injector temperature (°C)	100
Detector temperature (°C)	100
Current (mA)	70
Analysed gas	Hydrogen

Mole of hydrogen in y-axis and area reported by gas chromatography in x-axis are exhibited in the curves. The calibration curve of hydrogen is illustrated in the following Figure B.1.

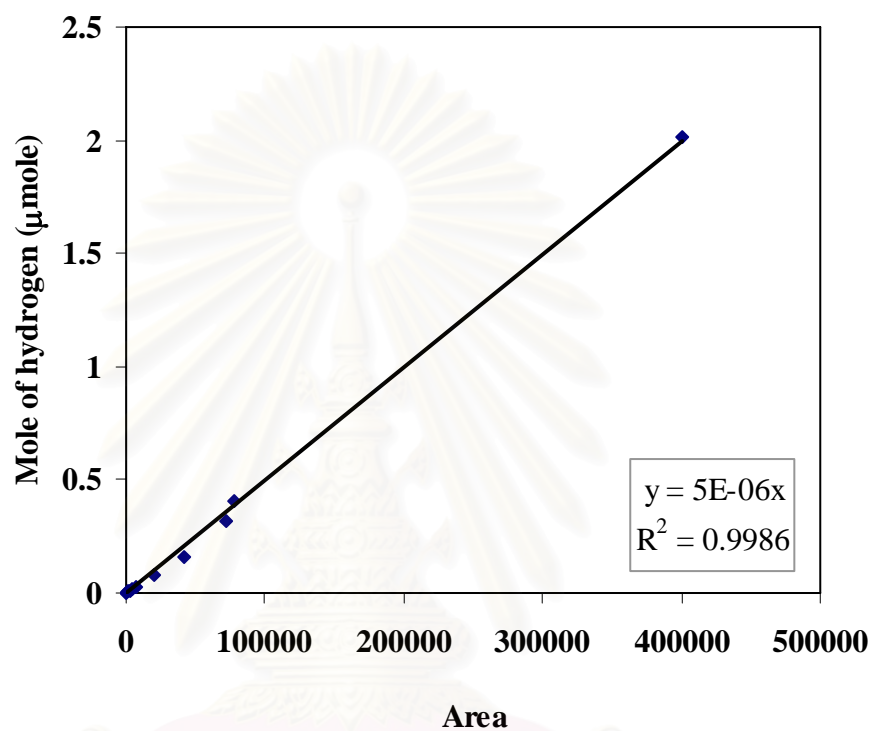


Figure B.1 The calibration curve of hydrogen

สถาบันวิทยบริการ
จุฬาลงกรณ์มหาวิทยาลัย

APPENDIX C

DETERMINATION OF Ti³⁺ SURFACE DEFECT FROM ESR MEASUREMENT

The amount of Ti³⁺ surface defects from ESR measurement can be relatively determined from:

$$\text{Ti}^{3+} \text{ surface defects} = \frac{\text{Intensity of ESR peak height}}{(\text{surface area}) \times (\text{catalyst weight})} \quad (\text{C.1})$$

Example: The amount of Ti³⁺ surface defects of titanium dioxide quenched in air at 77 K are determined as followed:

$$\text{Ti}^{3+} \text{ surface defect} = \frac{2670.0}{92.4 \times 0.081} = 356.7$$

Table C.1 The relative amount of Ti³⁺ surface defects of titanium dioxide quenched in various quenching media

Samples	Quenching media	Intensity of ESR peak height	BET surface area (m ² /g)	Weight (g)	Intensity of Ti ³⁺ surface defects per surface area
A	Air at 77 K	2670.0	92.4	0.081	356.7
B	Air at RT	2205.0	91.3	0.080	301.9
C	Air at 373 K	1765.0	88.2	0.081	247.4
D	30% wt H ₂ O ₂ at RT	1697.0	88.8	0.079	241.9
E	30% wt H ₂ O ₂ at 373 K	1353.0	94.2	0.080	179.5
F	H ₂ O at RT	1057.5	92.3	0.081	141.4
G	H ₂ O at 373 K	880.0	85.5	0.080	128.7

APPENDIX D

DATA OF CHARACTERIZATION OF Ti³⁺ SURFACE DEFECT FROM TEMPERATURE PROGRAM DESORPTION

Data of the characterization of Ti³⁺ surface defect from temperature program desorption (CO₂-TPD) can be shown:

Table D.1 The intensity peak of titanium dioxide quenched in various quenching media

Air at 77 K		Air at RT		Air at 373 K		30% wt H ₂ O ₂ at RT		30% wt H ₂ O ₂ at 373 K		H ₂ O at RT		H ₂ O at 373 K		TiO ₂	
Temp (K)	Intensity	Temp (K)	Intensity	Temp (K)	Intensity	Temp (K)	Intensity	Temp (K)	Intensity	Temp (K)	Intensity	Temp (K)	Intensity	Temp (K)	Intensity
100	1.4	100	1.4	100	1.4	100	1.4	100	1.4	100	1.4	100	1.4	100	1.4
110	1.5	110	1.4	110	1.5	110	1.4	110	1.4	110	1.4	110	1.5	110	1.4
120	1.5	120	1.5	120	1.5	120	1.5	120	1.5	120	1.5	120	1.5	120	1.6
125	1.7	125	1.7	125	1.8	125	1.7	125	2.4	125	1.7	125	2.0	125	2.0
135	2.7	130	3.0	130	2.8	130	3.0	130	3.7	130	2.9	130	3.6	130	4.4
140	3.5	140	5.5	135	3.8	135	4.5	135	5.2	140	6.0	135	4.9	135	5.5
150	6.4	150	6.8	140	5.0	140	5.5	140	6.0	150	6.7	140	5.5	140	5.6
155	7.0	155	7.5	145	6.0	150	7.0	150	6.7	155	7.2	150	6.5	145	6.7
160	7.7	160	8.3	150	6.7	155	8.0	155	7.3	160	8.2	155	7.2	150	7.1
165	8.5	165	8.8	160	7.9	160	8.5	160	8.2	165	8.5	160	8.0	155	7.8
170	8.9	170	8.6	165	8.4	165	8.7	165	8.4	170	8.4	165	8.2	160	8.5
180	8.3	180	8.0	170	8.8	170	8.3	175	7.7	175	8.0	170	8.0	165	8.8
185	7.9	185	7.6	175	8.5	175	7.7	185	7.2	180	7.5	175	7.5	175	8.2
188	7.9	190	7.9	180	8.0	182	7.2	190	7.7	185	7.3	182	6.9	180	7.8
190	8.0	195	8.1	185	7.7	190	7.5	195	7.8	190	7.5	190	7.2	185	7.5
195	8.4	200	7.8	190	7.8	195	7.6	200	7.4	195	7.7	195	7.3	190	8.0

Air at 77 K		Air at RT		Air at 373 K		30% wt H ₂ O ₂ at RT		30% wt H ₂ O ₂ at 373 K		H ₂ O at RT		H ₂ O at 373 K		TiO ₂	
Temp (K)	Intensity	Temp (K)	Intensity	Temp (K)	Intensity	Temp (K)	Intensity	Temp (K)	Intensity	Temp (K)	Intensity	Temp (K)	Intensity	Temp (K)	Intensity
198	8.5	205	7.3	196	8.4	200	7.3	205	6.6	200	7.5	205	6.6	195	8.3
205	8.0	210	6.6	205	7.5	210	6.0	210	6.2	210	6.3	210	6.1	200	6.3
210	7.0	225	5.0	210	6.9	225	4.8	220	5.0	225	4.8	225	4.7	210	6.3
225	5.0	240	4.0	225	5.0	240	3.9	240	3.8	240	3.8	240	3.8	225	5.0
250	3.5	250	3.5	240	3.9	250	3.5	250	3.3	250	3.5	250	3.4	240	3.8
260	3.1	260	3.2	255	3.1	265	3.0	260	3.0	260	3.1	260	3.1	250	3.4
280	2.7	275	2.8	285	2.5	285	2.6	275	2.7	275	2.7	275	2.8	280	2.7
300	2.4	295	2.5	300	2.4	300	2.4	300	2.4	300	2.4	300	2.4	300	2.5
310	2.4	310	2.4	310	2.4	310	2.4	310	2.4	310	2.4	310	2.4	310	2.4

สถาบันวิทยบริการ
จุฬาลงกรณ์มหาวิทยาลัย

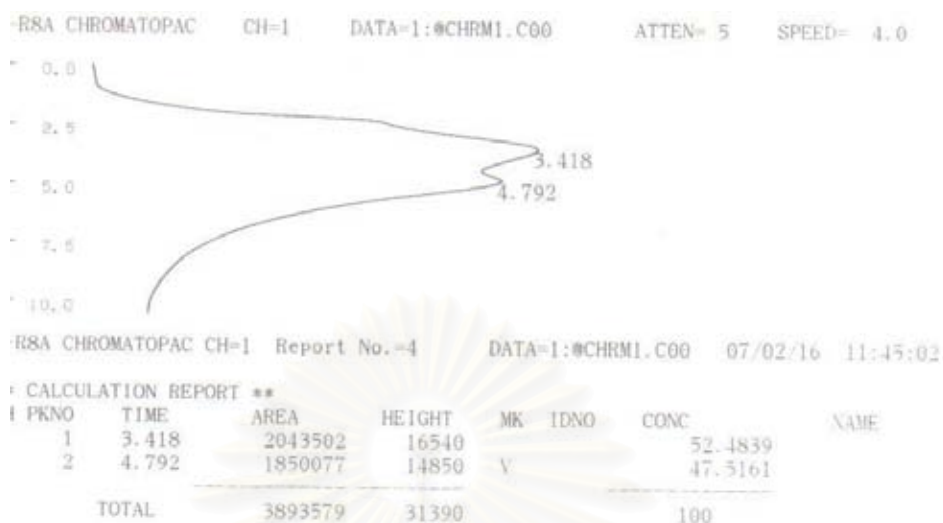


Figure D.1 Thermal desorption spectra for CO₂ adsorbed on TiO₂ quenched in air at 77 K from integrator

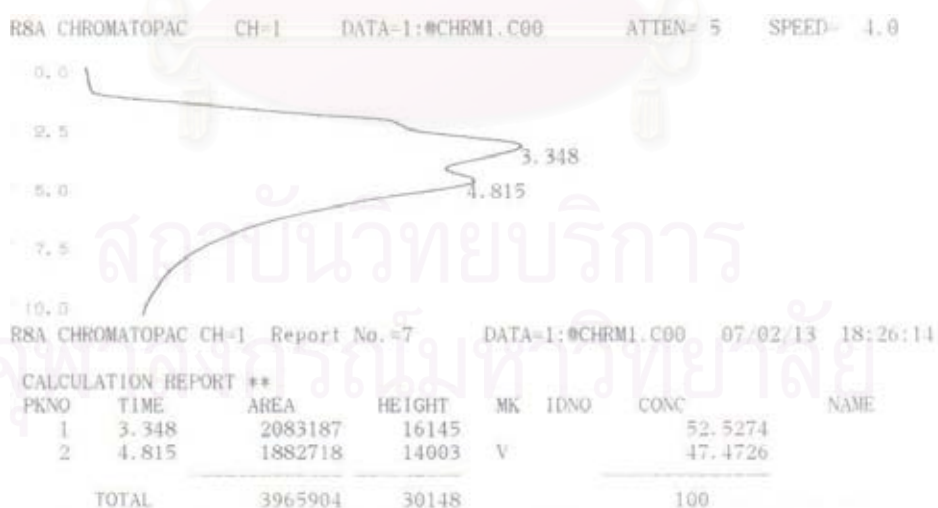


Figure D.2 Thermal desorption spectra for CO₂ adsorbed on TiO₂ quenched in air at RT from integrator

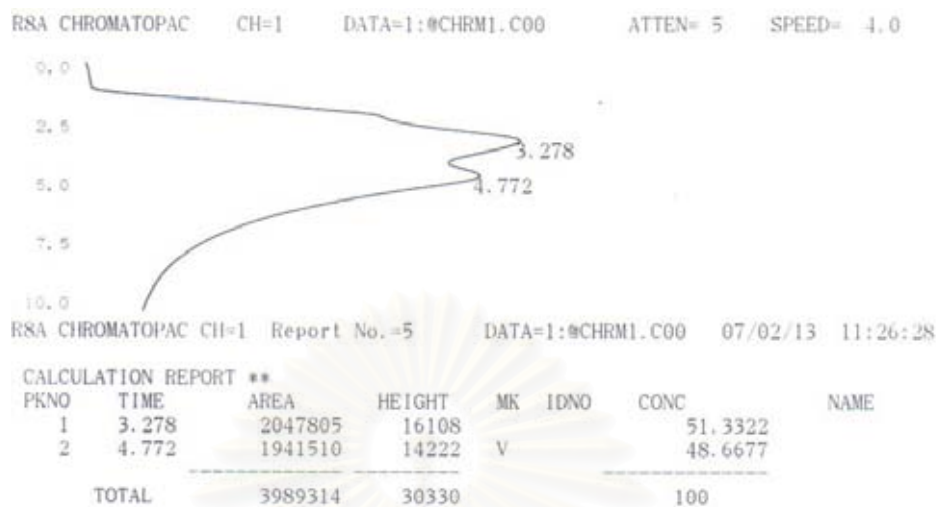


Figure D.3 Thermal desorption spectra for CO₂ adsorbed on TiO₂ quenched in air at 373 K from integrator

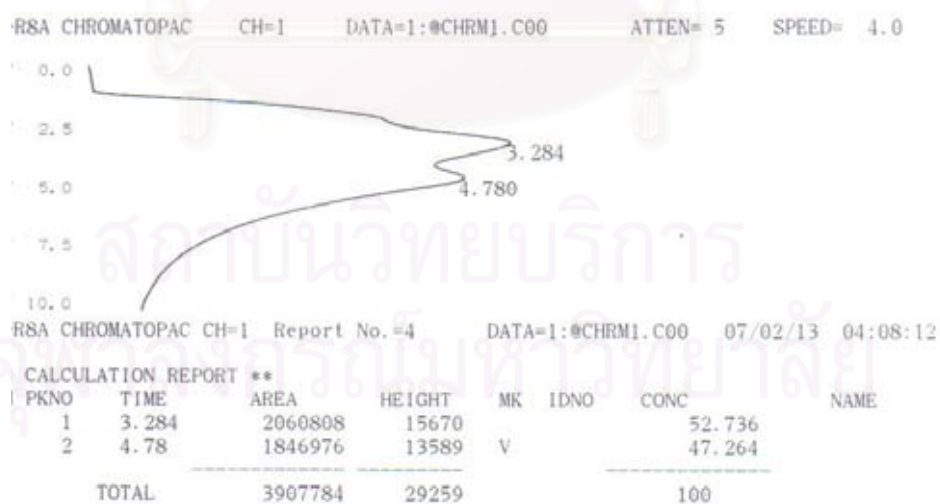


Figure D.4 Thermal desorption spectra for CO₂ adsorbed on TiO₂ quenched in 30% wt H₂O₂ at RT from integrator

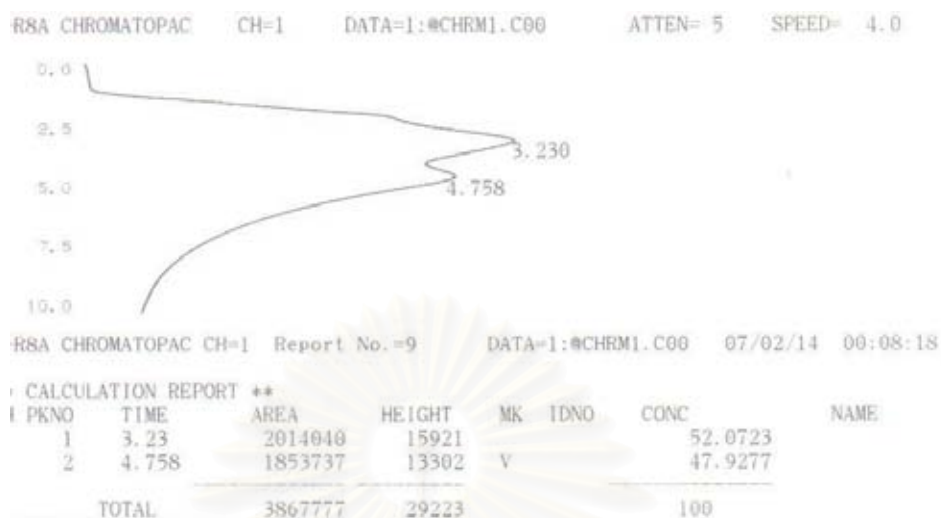


Figure D.5 Thermal desorption spectra for CO₂ adsorbed on TiO₂ quenched in 30% wt H₂O₂ at 373 K from integrator

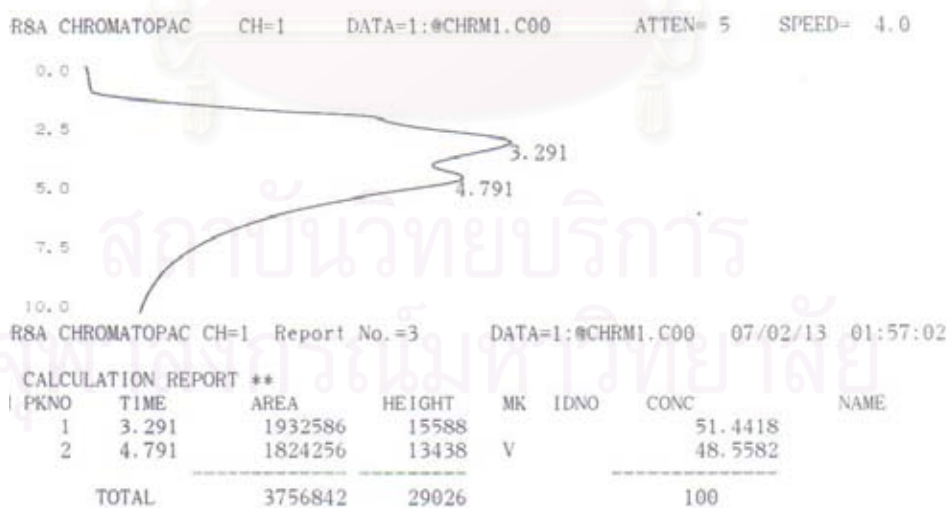


Figure D.6 Thermal desorption spectra for CO₂ adsorbed on TiO₂ quenched in H₂O at RT from integrator

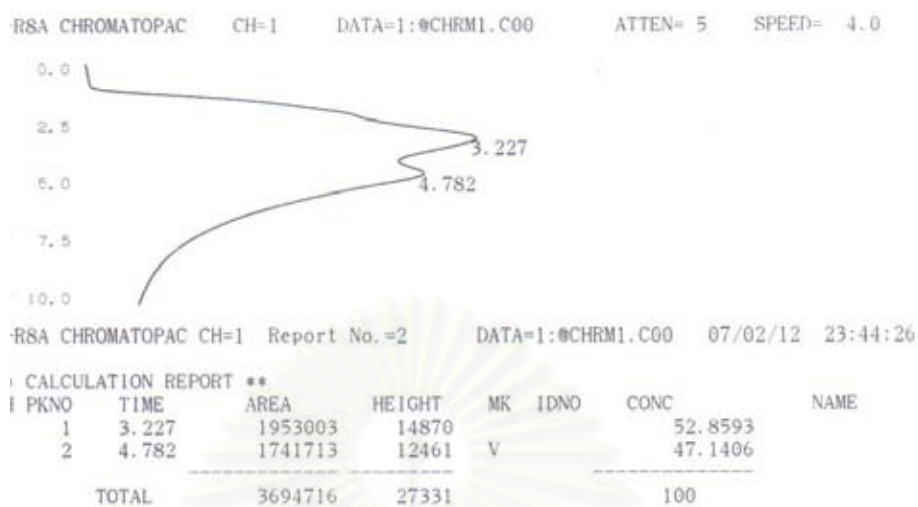


Figure D.7 Thermal desorption spectra for CO₂ adsorbed on TiO₂ quenched in H₂O at 373 K from integrator

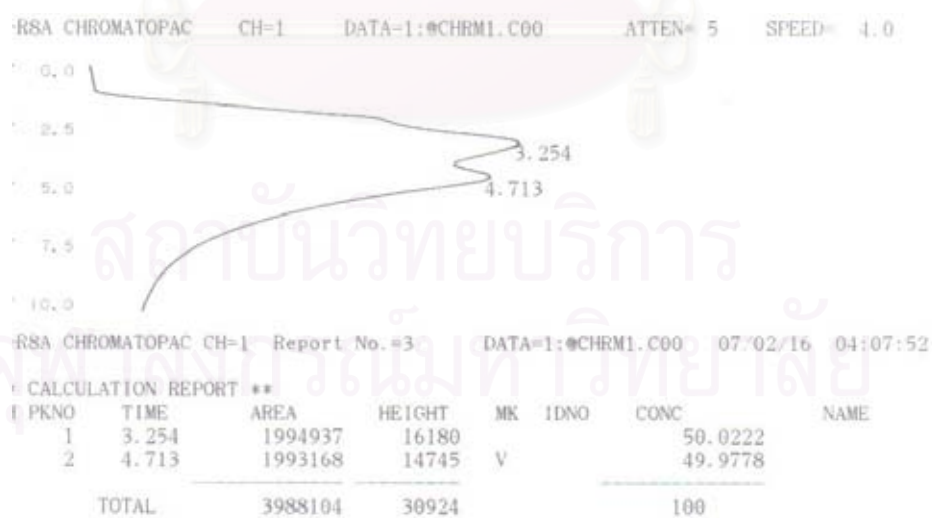


Figure D.8 Thermal desorption spectra for CO₂ adsorbed on TiO₂ from integrator

APPENDIX E

DATA OF PHOTOCATALYTIC REACTION FOR WATER DECOMPOSITION TO HYDROGEN

Data and results of photocatalytic reaction for water decomposition to hydrogen can be shown:

Table E.1 The data and results of photocatalytic reaction for water decomposition to hydrogen of titanium dioxide quenched in various media

Quenching in Air at 77 K					
Run. # 1			Run. # 2		
Time (min)	Peak area*	H ₂ production (μmole)	Time (min)	Peak area*	H ₂ production (μmole)
0	0	0	0	0	0
30	0	0	30	0	0
60	531	0.199	60	533	0.200
90	850	0.319	90	785	0.294
120	1052	0.395	120	1025	0.384
150	1132	0.425	150	1145	0.429
Quenching in Air at room temperature					
0	0	0	0	0	0
30	379	0.142	30	356	0.134
60	482	0.181	60	432	0.162
90	580	0.218	90	570	0.214
120	697	0.261	120	667	0.250
150	771	0.289	150	754	0.283

* Peak area from Gas Chromatograph (SHIMADZU GC-8A Molecular sieve 5A, TCD)

Quenching in Air at 373 K					
Run. # 1			Run. # 2		
Time (min)	Peak area*	H₂ production (μmole)	Time (min)	Peak area*	H₂ production (μmole)
0	0	0	0	0	0
30	0	0	30	0	0
60	434	0.163	60	474	0.178
90	507	0.190	90	547	0.205
120	612	0.230	120	652	0.245
150	695	0.261	150	735	0.276
Quenching in 30% wt H₂O₂ at room temperature					
0	0	0	0	0	0
30	0	0	30	0	0
60	471	0.177	60	488	0.183
90	535	0.201	90	519	0.195
120	583	0.219	120	569	0.213
150	634	0.238	150	659	0.247
Quenching in 30% wt H₂O₂ at 373 K					
0	0	0	0	0	0
30	0	0	30	0	0
60	471	0.177	60	491	0.184
90	544	0.204	90	519	0.195
120	553	0.207	120	579	0.217
150	659	0.247	150	647	0.253
Quenching in H₂O at room temperature					
0	0	0	0	0	0
30	0	0	30	0	0
60	434	0.163	60	404	0.152
90	486	0.182	90	456	0.171
120	568	0.213	120	538	0.202
150	622	0.233	150	592	0.222

Quenching in H₂O at 373 K					
Run. # 1			Run. # 2		
Time (min)	Peak area*	H₂ production (μmole)	Time (min)	Peak area*	H₂ production (μmole)
0	0	0	0	0	0
30	0	0	30	0	0
60	406	0.152	60	436	0.164
90	414	0.155	90	444	0.167
120	443	0.166	120	473	0.177
150	489	0.183	150	519	0.195
TiO₂ (not quenching)					
0	0	0	0	0	0
30	151	0.057	30	107	0.040
60	287	0.108	60	273	0.102
90	524	0.197	90	588	0.221
120	807	0.303	120	806	0.302
150	878	0.329	150	890	0.334

* Peak area from Gas Chromatograph (SHIMADZU GC-8A Molecular sieve 5A, TCD)

สถาบันวิทยบริการ
จุฬาลงกรณ์มหาวิทยาลัย

APPENDIX F

LIST OF PUBLICATIONS

1. Waraporn Chatpaisalsakul, Piyasan Prasertdam. “Effect of Surface Defect of Titanium Dioxide on Photocatalytic Activity for Water Decomposition to Hydrogen”, Regional Symposium on Chemical Engineering, Singapore, December 3-5, 2006.



สถาบันวิทยบริการ
จุฬาลงกรณ์มหาวิทยาลัย

Effect of Surface Defect of Titanium Dioxide on Photocatalytic Activity for Water Decomposition to Hydrogen

Waraporn Chatpaisalsakul^{a*}, Piyasan Praserttham^a

^a Center of Excellence on Catalysis and Catalytic Reaction Engineering, Department of Chemical Engineering, Chulalongkorn University, Bangkok 10330, Thailand

* Corresponding author: Tel. +66-02-2186711, Fax: +66-02-2186769, Email: waraporn_b@hotmail.com

ABSTRACT

Photocatalytic performance of water decomposition to hydrogen and oxygen has been studied by TiO₂ powder photocatalysts, which prepared by solvothermal method. Thus-obtained TiO₂ powder was treated to modify the surface properties by quenching in various media. The physical properties of TiO₂ samples were characterized by the many techniques such as Scanning Electron Microscope (SEM), surface area (BET) and X-ray diffraction (XRD). Surface defect structure of the thus-obtained TiO₂ samples was performed by using X-ray photoelectron spectroscopy (XPS) and CO₂ temperature programmed desorption (CO₂-TPD). The effect of quenching process on photocatalytic activity of TiO₂ powder was performed by using photocatalytic water decomposition to hydrogen as a model reaction. 0.3 g of TiO₂ was suspended in 40 mL of water in the 100 mL reaction cell. 10 mL of methanol was added as the sacrificial agent. The TiO₂ catalyst was suspended by magnetic stirring and irradiated with an UV lamp (60 W). The rates of evolution of hydrogen and oxygen were determined from gas products by gas chromatography (Shimadzu GC-8A (TCD), molecular sieve 5-Å column, Ar carrier). The effects of surface defect on the photocatalytic activity of TiO₂ were investigated.

1. INTRODUCTION

Titanium dioxide (TiO₂) in anatase phase has been recognized as one of the most important photocatalysts. Its photocatalytic activity is enhanced when the particle size approaches nanometer scale because of high surface area and short interface migration distances for photoinduced holes and electrons [1]. Nanocrystalline titania can be synthesized by many techniques. In this work, solvothermal method, which is the thermal decomposition of a metal alkoxide precursor in organic solvent, was employed. Titanium dioxide has been most widely used for studies of photocatalytic decomposition of water, because of its high stability against photocorrosion and its favorable band-gap energy. For H₂ production from water, many studies have concluded that direct photodecomposition of water into H₂ and O₂ has a very low efficiency due to rapid reverse reaction. A much higher hydrogen production rate can be obtained by addition of a "sacrificial reagent," such as alcohols, carbohydrates solid carbons, sulfide, etc [2].

2. MATERIALS AND METHODS

2.1 Preparation of the catalyst

Nanocrystalline TiO₂ was prepared using the solvothermal method. Titanium (IV) n-butoxide (purity 97 %, Aldrich) was used as the starting material. Approximately 25 g of titanium n-butoxide was suspended in 100 ml of toluene, in a test tube, which was then placed in a 300 ml autoclave. In the case of preparation modified TiO₂, a desired amount of the second metal precursor will be added into the test tube. The same solvent was filled in the gap between the test tube and the autoclave wall. The autoclave was purged completely by nitrogen after that it was heated up to the desired temperature at 300 K with the rate of 2.5 K/min. The temperature of the autoclave was held constant at 300 K for 2 h and then cooled down to room temperature. The obtained TiO₂ was washed by acetone for several times and finally dried in air.

For quenching pre-treatment, the synthesized TiO₂ was dried in air atmosphere at 300 K with a heating rate of 10 K/min for 1 h and then it was taken out and immediately quenched in various quenching media. In this study, gas phase media was used. For quenching in gas phase media, air at

room temperature and 77 K were selected. After the samples were quenched in the media for 30 min, all samples were dried in air at room temperature and stored in the desiccator

2.2 Photocatalytic reaction

The photocatalytic activity was determined by measuring the amount of hydrogen evolved from water splitting. About 0.3 g of TiO_2 was suspended in 40 mL of water in the 100 mL reaction cell. 10 mL of methanol was added as the sacrificial agent. The TiO_2 catalyst was suspended by magnetic stirring and irradiated by an UV lamp (60 W). The rates of evolution of hydrogen and oxygen were determined from gas products by gas chromatography (Shimadzu GC-8A (TCD), molecular sieve 5-Å column, Ar carrier).

RESULTS AND DISCUSSION

The XRD analysis of the obtained powder confirmed that the product was anatase titania without contamination from other crystalline phases. The crystallite size of all samples calculated from the Scherrer equation was approximately 11 nm. Surface area of all titania was also found to be roughly equal (c.a. $74 \text{ m}^2/\text{g}$). The results from XPS studies indicated mainly two types of surface properties. The air at 77 K quenched catalysts showed higher Ti binding energies than the air at room temperature quenched catalysts (Fig. 1). The binding energies of Ti ($459.7 \pm 0.2 \text{ eV}$ for Ti $2\text{P}_{3/2}$) for the air at room temperature and 77 K samples are typical of Ti^{4+} [2].

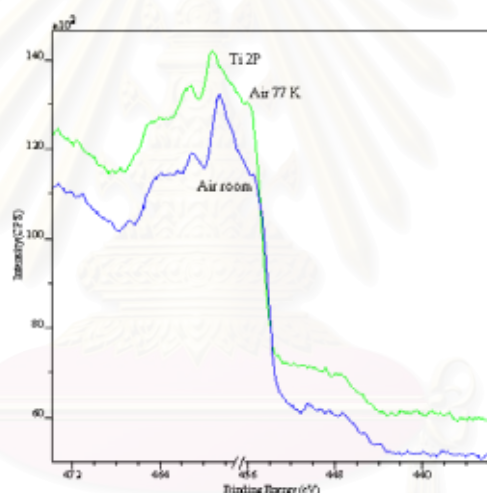


Fig. 1. XPS spectra of TiO_2 catalysts. Shown are Ti ($2\text{P}_{3/2}$) peaks. The lines are according to quenching in gas phase media.

The effects of surface defect on the photocatalytic activity of TiO_2 . As a result, an optimum density, as well as an optimum property, of the structure defect is expected for good photocatalysis performance.

CONCLUSION

In summary, TiO_2 powder photocatalysts, which prepared by solvothermal method. Obtained TiO_2 powder was treated to modify the surface properties by quenching in various media has been found to have significant effects on the photocatalytic activity of TiO_2 in hydrogen production from methanol/water solution. Quenching in air at 77 K, enhances visible-light excitation, leading to high activity.

REFERENCE

- [1] Tsai, S.J. and Cheng, S. (1997). *Effect of TiO_2 crystalline structure in photocatalytic degradation of phenolic contaminants*. Catal. Today. **33(1-3)**, 227-37.
- [2] Wu, N. L., Lee, M. S., Pon, Z. J., and Hsu, J. Z. (2004). *Effect of calcination atmosphere on TiO_2 photocatalysis in hydrogen production from methanol/water solution*. Journal of Photochemistry and Photobiology a-Chemistry, **163(1-2)**, 277-280.

VITA

Miss Waraporn Chatpaisalsakul was born on 27th December, 1983, in Pathum Thani, Thailand. She received her Bachelor degree in Chemical Engineering from the department of Chemical Engineering, Faculty of Engineering, Rangsit University, Pathum Thani, Thailand in March 2005. She continued her Master study in the major in Chemical Engineering at Chulalongkorn University, Bangkok, Thailand in June 2005.



สถาบันวิทยบริการ
จุฬาลงกรณ์มหาวิทยาลัย